



New Insights Into the Evolution of C₄ Photosynthesis Offered by the *Tarenaya* Cluster of Cleomaceae

Daniele F. Parma¹, Marcelo G. M. V. Vaz¹, Priscilla Falquetto¹, Jéssica C. Silva², Wellington R. Clarindo², Philipp Westhoff³, Robin van Velzen⁴, Urte Schlüter⁵, Wagner L. Araújo¹, M. Eric Schranz⁴, Andreas P. M. Weber⁵ and Adriano Nunes-Nesi^{1*}

¹ Departamento de Biologia Vegetal, Universidade Federal de Viçosa, Viçosa, Brazil, ² Departamento de Biologia Geral, Universidade Federal de Viçosa, Viçosa, Brazil, ³ Plant Metabolism and Metabolomics Laboratory, Cluster of Excellence on Plant Sciences, Heinrich Heine University Düsseldorf, Düsseldorf, Germany, ⁴ Biosystematics Group, Wageningen University & Research, Wageningen, Netherlands, ⁵ Institute of Plant Biochemistry, Cluster of Excellence on Plant Science, Heinrich Heine University Düsseldorf, Düsseldorf, Germany

OPEN ACCESS

Edited by:

Alistair McCormick,
University of Edinburgh,
United Kingdom

Reviewed by:

Xinguang Zhu,
Center for Excellence in Molecular
Plant Sciences, Chinese Academy
of Sciences (CAS), China
Karine Prado,
Carnegie Institution for Science (CIS),
United States

*Correspondence:

Adriano Nunes-Nesi
nunesnesi@ufv.br

Specialty section:

This article was submitted to
Plant Physiology,
a section of the journal
Frontiers in Plant Science

Received: 10 August 2021

Accepted: 16 December 2021

Published: 18 January 2022

Citation:

Parma DF, Vaz MGMV,
Falquetto P, Silva JC, Clarindo WR,
Westhoff P, van Velzen R, Schlüter U,
Araújo WL, Schranz ME, Weber APM
and Nunes-Nesi A (2022) New
Insights Into the Evolution of C₄
Photosynthesis Offered by
the *Tarenaya* Cluster of Cleomaceae.
Front. Plant Sci. 12:756505.
doi: 10.3389/fpls.2021.756505

Cleomaceae is closely related to Brassicaceae and includes C₃, C₃-C₄, and C₄ species. Thus, this family represents an interesting system for studying the evolution of the carbon concentrating mechanism. However, inadequate genetic information on Cleomaceae limits their research applications. Here, we characterized 22 Cleomaceae accessions [3 genera (*Cleoserrata*, *Gynandropsis*, and *Tarenaya*) and 11 species] in terms of genome size; molecular phylogeny; as well as anatomical, biochemical, and photosynthetic traits. We clustered the species into seven groups based on genome size. Interestingly, despite clear differences in genome size (2C, ranging from 0.55 to 1.3 pg) in *Tarenaya* spp., this variation was not consistent with phylogenetic grouping based on the internal transcribed spacer (ITS) marker, suggesting the occurrence of multiple polyploidy events within this genus. Moreover, only *G. gynandra*, which possesses a large nuclear genome, exhibited the C₄ metabolism. Among the C₃-like species, we observed intra- and interspecific variation in nuclear genome size as well as in biochemical, physiological, and anatomical traits. Furthermore, the C₃-like species had increased venation density and bundle sheath cell size, compared to C₄ species, which likely predisposed the former lineages to C₄ photosynthesis. Accordingly, our findings demonstrate the potential of Cleomaceae, mainly members of *Tarenaya*, in offering novel insights into the evolution of C₄ photosynthesis.

Keywords: Cleomaceae, *Cleoserrata*, genome size, *Gynandropsis*, intermediate photosynthetic mechanism, polyploidy, *Tarenaya*

INTRODUCTION

C₄ photosynthesis is a complex trait with a high degree of natural variation. It has evolved independently over 60 times in 19 different botanical families, involving anatomical and biochemical changes relative to the ancestral C₃ state (Sage, 2004; Sage et al., 2011, 2014). Accordingly, the different origins of this photosynthetic mechanism have been tracked by means of molecular markers (Patchell et al., 2014; Bayat et al., 2018), anatomical traits (e.g., different types of Kranz anatomy; Koteyeva et al., 2011), and biochemical patterns (three types of decarboxylation

enzymes; Hatch, 1988; Wang et al., 2014). In addition, the transition from C₃ to C₄ photosynthesis did not likely proceed through a single step, but rather *via* a series of transitory stages (Sage, 2004; Gowik and Westhoff, 2011; Schuler et al., 2016). These include the development of larger bundle sheath cells (BSCs), increase in leaf venation density (VD), restriction of glycine decarboxylase to BSCs, establishment of a photorespiratory carbon pump, enhancement of phosphoenolpyruvate carboxylase activity, establishment of the C₄ cycle, and optimization of the C₄ syndrome (Sage, 2004; Gowik and Westhoff, 2011). In this way, plants exhibiting C₃–C₄ intermediate characteristics bridge the evolutionary gap between the C₃ and C₄ species (Heckmann et al., 2013; Mallmann et al., 2014; Bräutigam and Gowik, 2016). Furthermore, phylogenetic studies have shown that many C₃–C₄ plants are closely related to C₄ plants (McKown et al., 2005; Marshall et al., 2007; Christin et al., 2011a; Kadereit and Freitag, 2011; Patchell et al., 2014).

Cleomaceae species have been used as model to study the evolution of C₄ photosynthesis, as this family comprises representatives of the three photosynthetic types (C₃, C₃–C₄ intermediates, and C₄) (Brown et al., 2005; Marshall et al., 2007). Additionally, Cleomaceae is closely related to Brassicaceae (sister families), which includes the C₃ model plant *Arabidopsis thaliana*. Accordingly, the genomes of species in these families show significant synteny (Schranz and Mitchell-Olds, 2006), and this close relationship has facilitated the identification of Cleomaceae orthologs in *A. thaliana*. Cleomaceae comprises nearly 200 species (Stevens, 2001; Bayat et al., 2018), three of which have been characterized as C₄ (*Gynandropsis gynandra*, *Coalisina angustifolia*, and *Areocleome oxalidea*), one as a C₃–C₄ intermediate (*Coalisina paradoxa*), and the rest as C₃ or C₃-like species (Marshall et al., 2007; Voznesenskaya et al., 2007; Koteyeva et al., 2011; Bayat et al., 2018). The three Cleomaceae members characterized as C₄ species have independent origins, as supported by phylogenetic (Patchell et al., 2014), anatomical (Koteyeva et al., 2011, 2014), and physiological evidence (Voznesenskaya et al., 2018). Therefore, this family is promising for obtaining a deeper understanding of the evolution of C₄ photosynthesis. However, despite of that, only 15 Cleomaceae species have been thoroughly characterized as yet (Marshall et al., 2007; Voznesenskaya et al., 2007; Koteyeva et al., 2011; Bayat et al., 2018).

Furthermore, some C₃ species of Cleomaceae deviate from the canonical C₃ state, exhibiting variable traits associated with the C₄ mechanism, such as increase in leaf VD, enlargement of BSCs, proliferation of both mitochondria and chloroplasts, and accumulation of transcripts and proteins required for C₄ photosynthesis, similar to C₃–C₄ intermediate and C₄ species (Marshall et al., 2007). These deviations indicate that these species may have a higher propensity for the evolution of C₄ photosynthesis (Marshall et al., 2007), facilitating the acquisition of novel traits (Sage, 2001; Marshall et al., 2007; McKown and Dengler, 2007; Christin et al., 2011b, 2012a,b, 2013), as observed in grasses (Christin et al., 2013). Of note, Cleomaceae species exhibiting C₃ (*Tarenaya hassleriana*) and C₄ (*G. gynandra*) photosynthetic metabolism share the copy number of various genes essential for C₄ photosynthesis. However, expression

analysis of C₄ photosynthetic orthologs have demonstrated that the regulation of transcript abundance is much less stringent in *T. hassleriana* than in *G. gynandra* (Bergh et al., 2014). Thus, compared with Brassicaceae, Cleomaceae species are expected to be predisposed to the evolution of C₄ photosynthesis, as already demonstrated for *G. gynandra* (Huang et al., 2021), given the evolutionary history of the group, including the occurrence of ancient whole genome duplications (Th- α) and paleopolyploidy events (Bergh et al., 2014).

As stated above, Cleomaceae species with C₄ photosynthesis have independent origins. The *Coalisina* group includes C₃, C₄, and C₃–C₄ intermediate species while *Gynandropsis* and *Areocleome*, do not, since they are monotypic genera (Patchell et al., 2014; Bayat et al., 2018). In this context, additional genera/species of the family need to be characterized, as species/accessions with different photosynthetic metabolisms within the same group may facilitate the understanding of the acquisition/evolution of the C₄ metabolism (Bayat et al., 2018). Although *G. gynandra* – the best-studied C₄ species of Cleomaceae – does not have a close C₃ or C₃–C₄ intermediate relative, studies with different accessions of this species have proven the presence of variations in the C₄ metabolism (Reeves et al., 2018). As consequence, variations in the C₃ and C₃–C₄ metabolism are also expected in other specious Cleomaceae genus, such as *Tarenaya*. Accordingly, establishment of a mapping population enables molecular marker trait association using methods such as quantitative trait locus mapping and genome-wide association studies (Reeves et al., 2018).

Despite the greatest species diversity (Stevens, 2001), few Cleomaceae species have been sampled for physiological traits to date. Brazil, for instance, is home to 34 Cleomaceae species (Bercht and Presl, 2021), most of which are endemic, but no species/accession has been physiologically characterized thus far. However, previous carbon isotope composition analysis has demonstrated the potential of this family to comprise species with the C₄ metabolism (e.g., *T. siliculifera*, a Brazilian endemic species) (Voznesenskaya et al., 2007). Considering that Brazil has a great diversity of Cleomaceae species and presents a wide range of biomes, including (semi)arid regions, that would favor the development of species with different carbon concentrating mechanisms, we tested the hypothesis that Brazilian Cleomaceae species, sampled from different areas, are in different steps/stages of C₃–C₄ evolution. Beyond to this basal hypothesis, we also intended to characterize and identify the type of photosynthetic metabolism in Brazilian Cleomaceae species and, thus, gaining insights into the evolution of C₃–C₄ intermediates and C₄ accessions in this family. For that, we investigated the phenotypic variability in terms of physiological (gas exchange), anatomical (diaphanization and cross section), and metabolic (sugars, starch, nitrogen compounds, and organic acids) traits. In addition, we measured the genome size of the studied species and reconstructed a molecular phylogeny based on the internal transcribed spacer (ITS) nuclear marker. In this context, we evaluated 22 phenotypically diverse accessions of Cleomaceae [distributed in 3 genera (*Cleoserrata*, *Gynandropsis*, and *Tarenaya*) and 11 species]. Accordingly, we have addressed a large number of *Tarenaya* species/accessions (the most specious

Cleomaceae genus in Brazil), including species of all its series. The results are, therefore, discussed in the context of the C₃–C₄ and C₄ evolutionary aspects of Cleomaceae, mainly considering *Tarenaya* species/accessions, highlighting the importance of this genus for studies on different carbon concentrating mechanisms.

MATERIALS AND METHODS

Taxon Sampling

For a subset of 22 Cleomaceae species selected for the present study, comprising herbaceous and shrub species, seeds were collected *in situ* from 20 locations distributed in 11 Brazilian states (Figure 1 and Supplementary Table S1). The species used in this study were sampled from four Brazilian biomes (Amazon, Atlantic Forest, Cerrado, and Caatinga, or transitional areas between these two last) (Figure 1 and Supplementary Table S1). These biomes differ from each other mainly by the predominant climate and vegetation. Thus, the Amazon Forest has a hot and humid climate, with dense vegetation characterized by large trees. The Cerrado (Brazilian Savanna), however, has a predominantly seasonal tropical climate, with periods of rain and drought, and vegetation characterized by gnarled trees, grasses and shrubs. The Caatinga (Brazilian semi-arid region), in turn, has a semi-arid tropical climate and medium-sized shrubby vegetation, with twisted branches and leaves adapted to periods of drought. The Atlantic Forest, on the other hand, has a predominantly tropical-humid climate with high temperatures and rainfall and vegetation

marked by the presence of large and medium-sized trees forming a dense and closed forest (IBGE, 2021).

After morphological identification, seven accessions were classified as *T. hassleriana* (shrub species), collected from different environments [locations: Viçosa, São Miguel do Anta, Canaã, and Piau in the state of Minas Gerais (MG); Domingos Martins in the state of Espírito Santo (ES); and Joinville and Canoinhas in the state of Santa Catarina (SC)]. Six accessions were classified as *T. longicarpa* (shrub species), collected from different environments [locations: Manaus in the state of Amazonas (AM); Ibimirim, Afrânio and Arcoverde in the state of Pernambuco (PE); Picos in the state of Piauí (PI); and Lavras in the state of Ceará (CE)]. The other species were classified as *C. paludosa* (shrub species) and *T. microcarpa* (herb species), which were collected from Belém in the state of Pará (PA); *T. aculeata* (herb species) and *T. diffusa* (herb species) collected from Feira de Santana in the state of Bahia (BA); *T. rosea* (shrub species) collected from Colatina (ES); *T. spinosa* (shrub species) collected from Teresina (PI); *T. parviflora* (shrub species) collected from Pombal in the state of Paraíba (PB); *T. siliculifera* (shrub species) collected from Rio Pardo (MG); and *G. gynandra* (herb species) collected from Mossoró in the state of Rio Grande do Norte (RN) (Figure 1 and Supplementary Table S1). The exsiccates are deposited in the VIC herbarium of the Universidade Federal de Viçosa (UFV).

The studied genera can be easily distinguished based on their morphological traits. *Cleoserrata* species are herbs with a glabrous surface, bearing leaves with three leaflets but

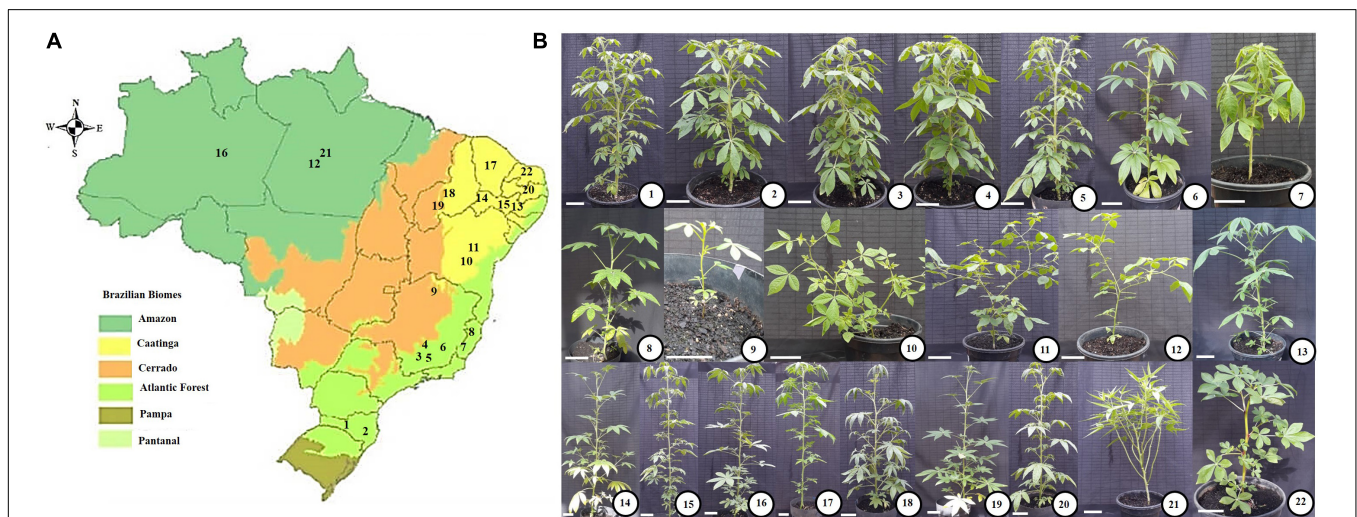


FIGURE 1 | Map of Brazil with its biomes (A) and pictures of the studied species (B). (A) Map showing the Brazilian biomes, in which the sampling sites of the studied species are highlighted by numbers (following the description presented in B). Accessions 1–8 were sampled from sites at Atlantic Forest; Accession 9 from Cerrado (Brazilian Savanna); Species 10, 11, 13–15, 17, 20, and 22 from Caatinga (Brazilian semi-arid region); Accessions 18 and 19 from transitional regions between Cerrado and Caatinga; Accessions 12, 16, and 21, from Amazon. (B) Pictures of the studied species, cultivated under greenhouse conditions (Please, see sections “Materials and Methods – Plant growth conditions”). (1) THCS: *T. hassleriana* (Canoinhas-SC). (2) THJ: *T. hassleriana* (Joinville-SC). (3) THV: *T. hassleriana* (Viçosa-MG). (4) THC: *T. hassleriana* (Canaã-MG). (5) THS: *T. hassleriana* (São Miguel-MG). (6) THP: *T. hassleriana* (Piau-MG). (7) THDM: *T. hassleriana* (Domingos Martins-ES). (8) TR: *T. rosea* (Colatina-ES). (9) TSI: *T. siliculifera* (Rio Pardo-MG). (10) TD: *T. diffusa* (Feira de Santana-BA). (11) TA: *T. aculeata* (Feira de Santana-BA). (12) TM: *T. microcarpa* (Belém-PA). (13) TIB: *T. longicarpa* (Ibimirim-PE). (14) TAF: *T. longicarpa* (Afrânio-PE). (15) TARC: *T. longicarpa* (Arcoverde-PE). (16) TAM: *T. longicarpa* (Manaus-AM). (17) TC: *T. longicarpa* (Lavras-CE). (18) TL: *T. longicarpa* (Picos-PI). (19) TS: *T. spinosa* (Teresina-PI). (20) TP: *T. parviflora* (Pombal-PB). (21) CP: *C. paludosa* (Belém-PA). (22) GG: *G. gynandra* (Mossoró-RN). The acronyms are followed by the species name and city/state of sampling, which are displayed between parentheses. Bars: 10 cm.

without stipules, ebracteate inflorescences, and large smooth black seeds. *Gynandropsis* species are annual herbs with a puberulent-glandular surface, bearing leaves with three to five leaflets, ebracteate inflorescences, and small smooth black seeds. Meanwhile, *Tarenaya* species are herbs or shrubs with a puberulent-glandular or pubescent surface, bearing three to seven foliolate leaves with epinescent stipules, bracteate inflorescences, and seeds with longitudinal and transverse streaks that are not very well developed (Stevens, 2001; Bercht and Presl, 2021).

Furthermore, the different *Tarenaya* species in Brazil can also be easily distinguished from one another. *T. aculeata* bears tree foliolate leaves, small white petals, and slightly moniliform capsules; *T. diffusa* bears three to five foliolate leaves, small white petals, and fusiform capsules; *T. microcarpa* bears three to five foliolate leaves, glandular-puberulent indumentum, and small purplish petals; *T. hassleriana* bears armed petioles, glandular-puberulent indumentum, spines on the veins, and pink flowers; *T. parviflora* bears glabrescent indumentum, three to seven foliolate leaves, armed petioles, and white to deep pink petals; *T. longicarpa* bears glandular-puberulent indumentum, completely white petals or petals white at base and purple at the apex (depending on accession), and long capsules, with the fruit being two to three times longer than the gynophore (which differs from *T. spinosa*); *T. spinosa* bears glandular-puberulent indumentum and small white petals (compared with *T. longicarpa*); *T. rosea* bears glandular-puberulent indumentum and petals white at base and pink at apex; and *T. siliculifera* bears glandular-puberulent indumentum without stipular spines, small white petals, obovoid capsules (almost all species of the genus have cylindrical fruits). The different accessions of *T. hassleriana* and *T. longicarpa* could also be distinguished from one another based on height, hairiness, spine density and disposition, and inflorescence as well as flower size.

Plant Growth Conditions

The collected seeds were germinated in 5 L plastic containers, filled with a commercial substrate supplemented with 14 g of NPK (4:14:8) per pot [0.56 g of N, 0.86 g of P₂O₅, and 0.93 g of K₂O]. During spring and summer, five plants of each accession were grown in a greenhouse under semi-controlled conditions (maximum photosynthetically active radiation of 1,500 μmol photons m⁻² s⁻¹, relative air humidity of 60%, and temperature of 30 ± 2°C) and were irrigated daily. Under these conditions, the plants were grown for 2 (herbaceous species) to 5 months (shrubby species) until physiological characterization and harvesting of leaf material for anatomical and biochemical analyses.

DNA Extraction, Amplification, and Sequencing

Total DNA was extracted from 22 fresh samples using a modified CTAB method (Doyle and Doyle, 1990). For phylogenetic analyses, the ITS regions were sequenced using the universal primers ITS 1 and ITS 4, as previously described (White et al., 1990). The fragments of interest were amplified

using polymerase chain reaction (PCR). PCR products were visualized using 1% agarose gel electrophoresis, isolated, and cleaned with the Wizard SV Gel and PCR Clean-Up System (Promega). The purified fragments were then sequenced (Myleus; Belo Horizonte, Brazil). The electropherograms were visually assessed, edited, base-called, assembled, and manually aligned using Sequencer 4.1 (GeneCodes, Ann Arbor, MI, United States).

We, therefore, performed a comprehensive phylogenetic analysis by adding the ITS sequences from Cleomaceae species, recovered from the National Center for Biotechnology Information (NCBI) (**Supplementary Table S2**), which has shown promise for the family in previous works (see Patchell et al., 2014; Reeves et al., 2018; Soares-Neto et al., 2020). Based on these sequences, we generated a matrix with 135 taxa (648 bp in length). The results were interpreted using Bayesian inference (BI). BI analyses were performed in MrBayes using the best-fit evolutionary model, selected according to the Akaike information criterion (Posada and Buckley, 2004), with MrModeltest 2.2 (Nylander, 2004). The Markov chain Monte Carlo algorithm was executed using four runs with 50 million generations each and sampling every 5,000 generations. The first 25% trees were discarded as burn-in. The remaining trees were used to construct the majority rule consensus tree, and the posterior probability (PP) for each node was calculated.

Flow Cytometry

Leaf fragments (~2 cm²) from each Cleomaceae accession (sample) and *Solanum lycopersicum* (internal standard, 2C = 2.00 pg; Praça-Fontes et al., 2011) were co-chopped in 0.5 mL of OTTO-I nuclear extraction buffer (Otto, 1990) supplemented with 2 mM dithiothreitol and 50 μg mL⁻¹ RNase (Praça-Fontes et al., 2011). Then, 0.5 mL of the same buffer was added, and the suspensions were filtered through a 30 μm nylon mesh, placed into a microtube, and centrifuged at 100 × g for 5 min. The precipitate was resuspended in 100 μL of OTTO-I buffer and incubated for 10 min. The suspensions were stained with 1.5 mL of OTTO-I:OTTO-II (1:2) buffer supplemented with 2 mM dithiothreitol, 75 μg mL⁻¹ propidium iodide, and 50 μg mL⁻¹ RNase (Praça-Fontes et al., 2011). The suspensions were incubated in the dark for 30 min, filtered through a 20 μm nylon mesh, and analyzed using a flow cytometer (BD Accuri C6, Accuri Cytometers, Belgium) equipped with a 488 nm laser source to promote propidium iodide emission at FL2 (615 – 670 nm) and FL3 (>670 nm). Fluorescence peaks of the G₀/G₁ nuclei of each Cleomaceae accession and *S. lycopersicum* were analyzed based on histograms using BD AccuriTM C6. The G₀/G₁ nuclear peaks exhibiting a coefficient of variation of ≤5% were considered for genome size measurement, calculated as 2C_D = (C1/C2) × 2C_S, where 2C_D is the 2C value (pg) of each Cleomaceae accession, C1 is the mean G₀/G₁ peak channel of the Cleomaceae accession, C2 is the mean G₀/G₁ peak channel of *S. lycopersicum*, and 2C_S is 2.00 pg of *S. lycopersicum*. Based on previous results, the *S. lycopersicum* internal standard was replaced with *Raphanus sativus* 'Saxa' (2C = 1.13 pg, Praça-Fontes et al., 2011) to measure the 2C value of *G. gynandra* (GG, Mossoró-RN) and *T. siliculifera* (TSI, Rio Pardo-MG).

Carbon Isotope Composition Analysis

Leaf material was oven-dried at 60°C for 48 h and used to determine $\delta^{13}\text{C}$ and the C/N ratio. The material was analyzed using the Isoprime 100 isotope ratio mass spectrometer coupled to an isotope cube elemental analyzer (Elementar, Hanau, Germany), as described by Gowik and Bra (2011).

Gas Exchange and Fluorescence Analyses

Fully expanded leaves from the third node of non-flowering plants were used for gas exchange and chlorophyll *a* fluorescence analysis, which were carried out with an open-flow infrared gas exchange analyzer system equipped with an integrated fluorescence chamber (IRGA, LI-COR Inc. LI-6400XT; NE). The measurements were performed during the light period between 8 and 12 h (solar time), using a 2 cm² leaf chamber at 25°C, flow rate of 400 $\mu\text{mol CO}_2 \text{ s}^{-1}$ and saturating light intensity of 1,000 $\mu\text{mol photons m}^{-2} \text{ s}^{-1}$ at the leaf level. The leaf-to-air vapor pressure deficit was maintained at 1.2–2.0 kPa, and the amount of blue light was set to 10% PPFD to optimize the stomatal aperture. Corrections for CO₂ leakage into and water vapor from the leaf chamber of LI-6400 were applied to all gas exchange data, as previously described (Rodeghiero et al., 2007). Dark respiration (R_d) was measured using the same gas exchange system described above, on the same leaves used for determination of the gas exchange parameters, after at least 1 h of acclimation in the dark (Rodeghiero et al., 2007).

Metabolite Analyses

Fully expanded leaves from the third node of non-flowering plants were harvested in the middle of the light period, soon after gas exchange and fluorescence analyses. At this point, the herbaceous plants were 2-month-old and the shrub species were 5-month-old. The samples were snap-frozen and stored at –80°C until analysis. Metabolites were extracted by grinding the material in liquid nitrogen and adding the appropriate extraction buffers. Approximately 25 mg of the freeze-dried leaf matter was subjected to ethanolic extraction at 70°C for 30 min. After centrifugation (at 21,800 × *g* for 5 min), the total chlorophyll content (*a* + *b*) and chlorophyll *a/b* ratio were determined as previously described (Porra et al., 1989).

The concentration of glucose, fructose, and sucrose was determined from the liquid phase, as described previously (Fernie et al., 2001). Total free amino acid (Cross et al., 2006), malate, and fumarate (Nunes-Nesi et al., 2007) contents were determined as previously described. From the ethanol insoluble fraction, the concentration of starch (Fernie et al., 2001) and total soluble proteins (Bradford, 1976) was determined according to standard protocols.

Metabolite Profiling

Fully expanded source leaves from each sampled plant were collected in the middle of the light period, wrapped in aluminum foil, flash frozen in liquid nitrogen, and stored at –80°C until analysis. After lyophilization and grinding, approximately 15 mg dry weight was extracted for gas chromatography–mass

spectrometry (GC–MS) in 1.5 mL of extraction solution (water:methanol:chloroform, 1:2.5:1 *v/v*) as described by Fiehn (2007), using 5 μM ribitol (Sigma-Aldrich) as the internal standard. The extract (15 μL) was dried in a vacuum concentrator and derivatized in two steps using the MPS Dual Head autosampler (Gerstel), as described by Gu et al. (2012). After incubation for 2 h at room temperature, the samples were analyzed as described previously (Shim et al., 2020) using the 5977B GC-MSD system (Agilent Technologies). The peaks were integrated using MassHunter Quantitative (*v* b08.00; Agilent Technologies). For relative quantification, metabolite peak areas were normalized to the corresponding dry weight and peak area of the internal standard.

Micromorphological Analyses

Anatomical analysis was conducted to evaluate the VD of fully developed leaves in the upper third. Diaphanization of the plant material was performed as described previously (Zsögön et al., 2015). Subsequently, the samples were assembled on glass slides, and images of the adaxial epidermis were obtained using the Zeiss Axio Scope A1 photomicroscope coupled to a color image capture system (Axiovision® 105). Five photographs of each slide were obtained to cover the entire leaf length. In addition, five replicates (five leaves per individual) were collected and analyzed. Vein density was calculated as the length of the second-, third-, and fourth-order veins in a given leaf area (mm mm^{-2}). Quantification was performed using Image Pro-Plus® (*v* 4.5; Media Cybernetics, Silver Spring, MD, United States). In addition, the median region of the fully expanded leaves from the third node was collected and fixed in formaldehyde:acetic acid:ethanol 50% (FAA50) at a ratio of 5:5:9 (*v/v*) for 48 h. The material was dehydrated in an ethanolic series and embedded in historesin (Leica, Heidelberg, Germany). Transverse sections (thickness, 5 μm) were obtained using a self-advancing rotary microtome (RM 2155, Leica, Heidelberg, Germany) with glass razors. The sections were stained with 0.05% toluidine blue in acetate buffer (pH 4.7) (O'Brien et al., 1964) for 1 min and assembled between slides and coverslips with synthetic resin. Photomicrographs were obtained using a photomicroscope (Zeiss, MC-80). The micrometric scales were photographed and enlarged under the same optical conditions. Leaf thickness was measured considering the entire length of the epidermis. For each slide analyzed, five measurements were obtained in different regions to cover the entire area. The distance between the vascular bundles was measured between the sides of the veins. Bundle sheath cell width (BSCW) was measured radially in five cells at random on each slide (cells from different vascular bundles were selected when possible). Leaf thickness, palisade parenchyma, spongy parenchyma, intervein distance, and BSCW were measured (Supplementary Figure S1) using Image Pro-Plus®.

Statistical Analyses

Data were obtained from five plants per accession, each placed in an individual pot; thus, each pot represented a biological replicate. All plants were completely randomized. The effect of

accession was determined using analysis of variance ($P < 0.05$). Means were analyzed using Tukey's test.

Phylogenetic generalized least squares (PGLS) regression was applied. We used a phylogenetic tree constructed using BI based on the ITS sequences of 21 novel Brazilian accessions (**Supplementary Figure S2**) and a matrix of 74 variables. The species *G. gynandra* (C₄ species) was removed from the analysis, as its genome size values (2–4 times greater compared to the other species in this study) and results obtained from other analyzes could bias/influence the regression result. The script available at <https://lukejharmon.github.io/ilhabela/instruction/2015/07/03/PGLS/> was used. PGLS uses the common statistical mechanism of generalized least squares and applies it to phylogenetic comparative data (Felsenstein, 1985a). This method allows for the estimation of the impact of phylogeny on the covariance among residuals, thereby controlling for relatedness. In the case of Brownian motion, residues with variances and covariances follow the structure of the phylogenetic tree (Felsenstein, 1985b). All statistical analyses were performed using Statistica and R.

RESULTS

The Cleomaceae species selected for this study were sampled from 20 sites, which were found in four Brazilian biomes (Amazon, Atlantic Forest, Cerrado, and Caatinga) (**Figure 1** and **Supplementary Table S1**). In this sense, the biomes with the highest number of sampled specimens were the Atlantic Forest (11 spp.) and Caatinga (7 spp.). However, beyond the differences in climate and vegetation described above, these biomes also show great diversity considering its phytophysiological characteristics. Accordingly, the Atlantic Forest has 12 ecosystems/phytophysiological characteristics (IBGE, 2021) while Caatinga has six main phytophysiological characteristics (Andrade-Lima, 1981). Interestingly, it was also possible to observe that accessions of the same species (mainly *Tarenaya hassleriana* and *T. longicarpa*), collected from different sites showed phenotypic/morphological plasticity (**Figure 1**). More important, as described below, in addition to the phenotypic plasticity, accessions from different locations also displayed great genetic and physiological diversity.

Genome Size in Cleomaceae

In flow cytometry histograms with G₀/G₁ peaks of nuclear suspensions, the coefficient of variation for all Cleomaceae species/accession and the internal standards (*S. lycopersicum* or *R. sativus*) was < 3.70%. Based on genome size, the 22 accessions were separated into seven groups: (i) *T. hassleriana* accessions (THC, THCS, THDM, THJ, THP, THS, and THV) with 2C = 0.55 pg ± 0.003; (ii) *T. diffusa* (TD) with 2C = 0.59 pg ± 0.004; (iii) *T. aculeata* and *T. microcarpa* (TA and TM) with 2C = 0.66 pg ± 0.004; (iv) *T. siliculifera* (TSI) with 2C = 0.77 pg ± 0.003; (v) *C. paludosa* (CP) with 2C = 1.08 pg ± 0.004; (vi) nine *Tarenaya* species (TS, TP, TL, TR, TAF, TAM, TARC, TC, and TIB) with 2C = 1.30 pg ± 0.014; and (vii) *G. gynandra* (GG) with 2C = 2.20 pg ± 0.002 (**Figure 2A**). This pattern found for genome size

was somehow unexpected, mainly because most species belong to the same genus. Accordingly, indicating the high degree of variation, mainly of *Tarenaya* species/accessions, which are spread into five different groups. Thus, we observed intrageneric and interspecific variation in nuclear genome size among the Brazilian Cleomaceae species. Based on the mean 2C values and phylogeny (**Figure 2B**), we speculate that increase and decrease in genome size contributed to the diversification of Cleomaceae species, specifically the C₄ species *G. gynandra* (2C = 2.20 pg, fourfold higher than that of *T. hassleriana*). Considering the correlation between the 2C value and the 2n chromosome number of *Tarenaya* species and *G. gynandra*, we hypothesize that euploidy and dispoloidy (ascendant and/or descendant) resulted in interspecific variations in the 2C value and C₄ photosynthetic mechanism of *G. gynandra*. Alternatively, genome size differences may be attributable to whole genome duplications (Mabry et al., 2020) and/or changes in repetitive DNA content (Beric et al., 2020, 2021).

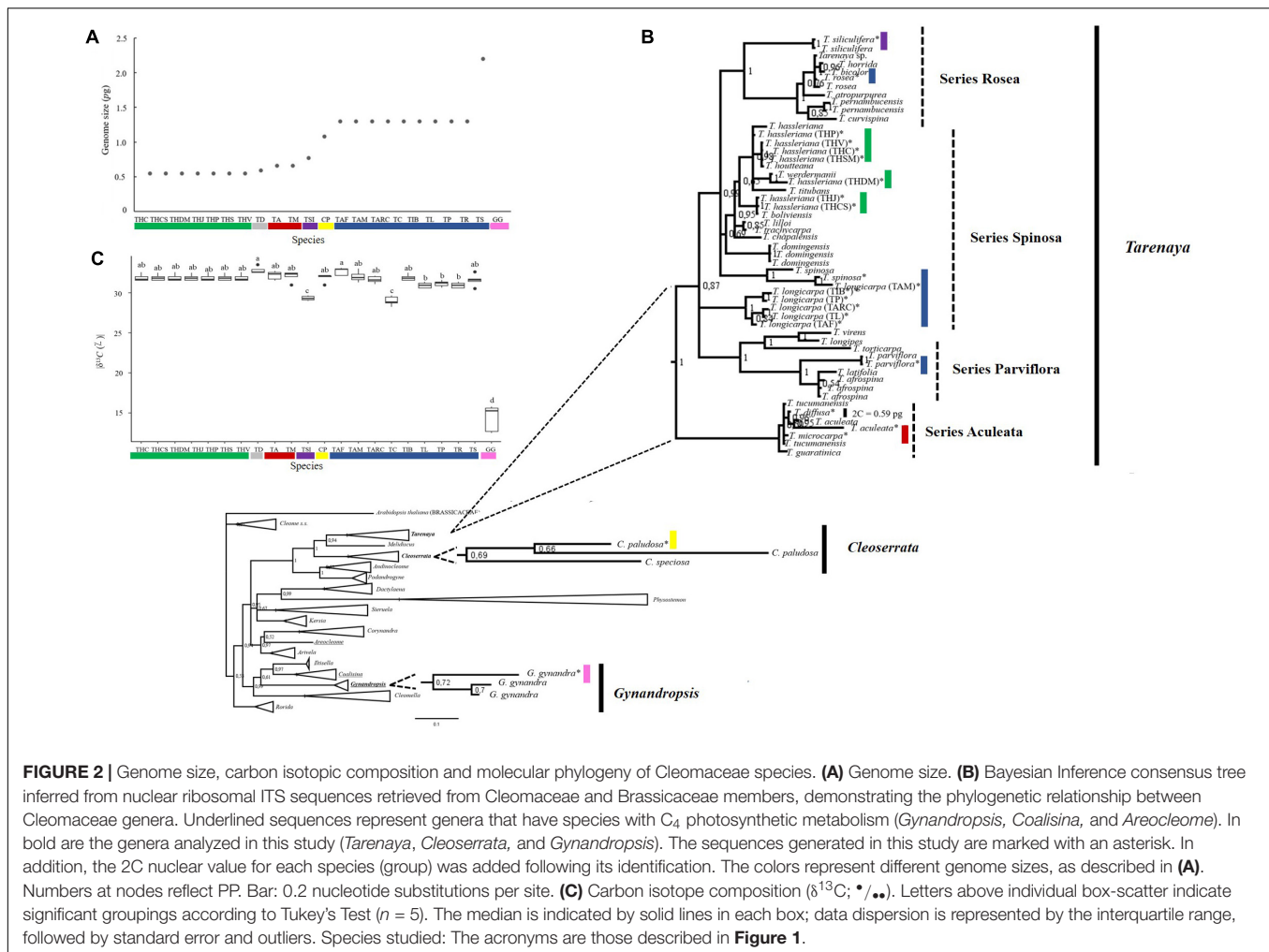
Phylogeny of Cleomaceae Accessions

Our Bayesian phylogenetic reconstruction based on the ITS sequences of Cleomaceae species indicated that most of our analyzed accessions were positioned in the *Tarenaya* genus. The exceptions were the sequences of *C. paludosa* and *G. gynandra*, which were placed into the *Cleoserrata* and *Gynandropsis* clusters, respectively (**Figure 2B**). Moreover, *Tarenaya* is sister to two American genera, namely *Cleoserrata* and *Melidiscus*, whereas *Gynandropsis* is sister to the African cluster comprising *Coalisina* and *Ittisella* as well as to *Cleomella* (**Figure 2B**). These results are somehow contrary to the findings reported by Bayat et al. (2018), who used five molecular markers (ITS, *matK*, *ndhF*, *ycF*, and *rps*) and another set of species/sequences. Interestingly, *Gynandropsis*, *Areocleome*, and *Coalisina*, which harbor species with C₄ photosynthetic metabolism, formed different clusters (**Figure 2B**), reinforcing that this photosynthetic mechanism has evolved independently at least three times within the family, as was previously reported (Patchell et al., 2014; Bayat et al., 2018).

The analyzed genera, namely *Gynandropsis*, *Cleoserrata*, and *Tarenaya* are monophyletic. Within the *Tarenaya* group, the series *Rosea*, *Parviflorae*, and *Aculeatae* are monophyletic; the *Spinosa* series, which includes the type species of the genus (*T. spinosa*), is polyphyletic; and the *Aculeatae* series, which includes herbaceous species bearing small flowers, is placed more externally to the other series of the genus (**Figure 2B**). Within the *Spinosa* series, *T. hassleriana* accessions form different sub-clusters, indicating high genetic diversity among the species (**Figure 2B**). Overall, the 20 accessions of *Tarenaya* studied here cover a great genetic diversity into this genus, mainly considering that species from all series were sampled and were represented in all analysis.

Carbon Isotope Composition

The carbon isotope composition of plants has been widely used to identify the photosynthetic mechanisms, and it can, therefore, assist phylogenetic studies exploring the evolution of C₄ photosynthesis (Von Caemmerer et al., 2014; Yang et al., 2017). Hence, to help identifying the photosynthetic mechanism



of the accessions studied here and to merge these data with molecular phylogeny, we performed carbon isotope composition ($\delta^{13}\text{C}$) analysis using fully expanded leaves of plants growing under the same conditions. In the Cleomaceae accessions tested, the $\delta^{13}\text{C}$ value ranged from -15‰ to -32‰ , representing at least two types of photosynthetic mechanisms, namely C₃ and C₄ (**Figure 2C**). As expected, the Brazilian accession of *G. gynandra* exhibited the highest $\delta^{13}\text{C}$ value (-15‰), and the other species showed values around -32‰ . Meanwhile, *T. siliculifera* and *T. longicarpa* (Lavras, CE) exhibited $\delta^{13}\text{C}$ values close to -29‰ , being significantly different from the other accessions (**Figure 2C**), highlighting a certain degree of variation among the C₃-like species found into the genus *Tarenaya*.

Phylogenetic Generalized Least Squares Regression

In order to determine the correlations of genome size with the other study variables, independently, in the phylogenetic topology of the Brazilian Cleomaceae accessions, we decided to perform PGLS regression analysis (**Table 1** and **Supplementary Figures S3, S4**). As the size of the *G. gynandra* genome is 2–4

times greater compared to the other species in this study, we removed this species from the analysis to avoid bias/influence the regression result.

It is noteworthy that a phylogeny, based on the studied species (except *G. gynandra*), was built exclusively for PGLS. Thus, with a smaller sample of species and a single molecular marker (ITS), it is possible to see that the *Tarenaya* series were no longer monophyletic (**Supplementary Figure S2**). PGLS analysis revealed that 32 out of 74 variables analyzed here were significantly correlated to genome size ($P < 0.05$) (**Table 1**). Based on the significant regressions, the models with gas exchange parameters (A_N , A_{gross} and R_D), leaf anatomical traits (size of palisade parenchyma and VD), organic acids (malate, isocitrate, and gluconate), amino acids (aspartate, α -alanine, methionine, phenylalanine, tyrosine, glutamine, serine, glycine, and leucine), other nitrogen-metabolism related compounds (γ -aminobutyric acid, GABA), putrescine and ornithine), total chlorophyll, glucose, and glycerol were positively correlated with genome size. Interestingly, the $\delta^{13}\text{C}$ value, intrinsic water use efficiency (WUE_i), malonate, myo-inositol, proline, starch content, proteins content, seeds weight and specific leaf area were negatively

TABLE 1 | Variables that were significant ($p < 0.05$) in PGLS model with genome size.

		Minimum	Mean	Maximum	SE	CV	Correlation	P		
Physiological parameters	A_N ($\mu\text{mol CO}_2 \text{ m}^{-2} \text{ s}^{-1}$)	7.31	19.56	31.86	0.73	0.17	+	0.003		
	R_d ($\mu\text{mol CO}_2 \text{ m}^{-2} \text{ s}^{-1}$)	0.70	1.37	1.80	0.06	0.21	+	0.01		
	WUE _i ($\mu\text{mol m}^{-2} \text{ s}^{-1}$)	29.65	44.15	77.59	2.57	0.27	-	0.001		
	A_{gross} ($\mu\text{mol CO}_2 \text{ m}^{-2} \text{ s}^{-1}$)	14.85	27.52	36.70	0.68	0.11	+	0.001		
Biochemical parameters	$ \delta^{13}\text{C} (\text{‰}) $	28.97	31.56	32.79	0.14	0.02	-	0.001		
	Proteins ($\mu\text{mol g}^{-1} \text{ DW}$)	6.63	8.91	13.53	0.28	0.15	-	0.001		
	Starch ($\mu\text{mol glucose g}^{-1} \text{ DW}$)	0.01	0.02	0.06	0.00	0.42	+	0.001		
	Chlorophyll $a + b$ ($\mu\text{mol g}^{-1} \text{ DW}$)	5.95	29.89	156.08	4.19	0.64	+	0.001		
Anatomical parameters	Palisadic parenchyma (μm)	7.76	14.23	17.58	0.48	0.15	+	0.001		
	Density of venation (mm mm^{-2})	15.95	24.99	48.79	1.17	0.22		0.018		
Metabolites data	Amino acids	α -Alanine	251.13	472.96	2226.79	41.53	0.40	+	0.001	
		Glutamine	0.04	0.06	0.11	0.00	0.13	+	0.001	
		Glycine	9.26	32.97	116.09	3.68	0.51	+	0.001	
		Leucine	5.14	45.59	110.89	6.32	0.64	+	0.001	
		Ornithine	0.05	0.07	0.12	0.00	0.13	+	0.042	
		Phenylalanine	54.55	174.23	541.60	17.05	0.45	+	0.031	
		Proline	55.46	130.42	210.29	7.70	0.27	-	0.001	
		Methionine	72.58	160.90	311.50	10.37	0.30	+	0.001	
		Putrescine	36.67	90.91	384.39	8.88	0.45	+	0.001	
		Serine	0.08	0.14	0.23	0.00	0.12	+	0.003	
	Organic acids	Tyrosine	492.03	1480.16	6638.51	165.25	0.51	+	0.01	
		Aspartate	3.36	21.66	93.91	2.98	0.63	+	0.001	
		GABA	236.29	382.87	1116.21	27.38	0.33	+	0.005	
		Gluconate	17.61	54.62	229.72	4.85	0.41	+	0.001	
		Glycerol	16.80	53.39	114.24	4.94	0.42	+	0.001	
		Isocitrate	1239.68	7818.80	37737.81	743.17	0.44	+	0.036	
		Malate	6.39	27.32	93.11	3.11	0.52	+	0.002	
		Malonate	431.45	1712.42	3809.49	157.24	0.42	-	0.003	
		Sugar	Glucose	15.32	104.02	1013.09	20.35	0.90	+	0.001
			Myo-Inositol	6.06	164.93	1257.78	31.70	0.88	+	0.003
Development	Specific leaf area ($\text{m}^2 \text{ mg}^{-1}$)	249.45	371.57	503.55	18.26	0.23	-	0.001		
	Weight 1000 seeds (g)	1.06	2.16	3.07	0.09	0.20	-	0.001		

The raw data are plotted with the phylogenetic generalized least squares regression line in **Supplementary Figures S2, S3**.

correlated with genome size (**Table 1** and **Supplementary Figures S3, S4**).

Physiological Parameters

To completely characterize and understand the physiological basis for the differences among the studied Cleomaceae accessions, we performed detailed physiological analyses of diffusional, photochemical, and biochemical constraints on photosynthesis (**Figures 3A–D** and **Supplementary Figure S5**). Under the tested environmental conditions (as described in the section “Materials and Methods”), Cleomaceae accessions showed natural variation, even within the same species, in terms of physiological parameters related to photosynthesis. In general, the studied Cleomaceae accessions exhibited a high A_N , with values greater than $20 \mu\text{mol CO}_2 \text{ m}^{-2} \cdot \text{s}^{-1}$ (**Figure 3A** and **Table 2**). However, the herbaceous accessions of *T. aculeata*, *T. diffusa*, and *T. microcarpa* exhibited the A_N of $\sim 10 \mu\text{mol CO}_2 \text{ m}^{-2} \cdot \text{s}^{-1}$. While the shrubby accession of *T. siliculifera* showed the A_N of $< 10 \mu\text{mol CO}_2 \text{ m}^{-2} \cdot \text{s}^{-1}$. *T. siliculifera* exhibited

the lowest stomatal conductance (g_s), followed by *G. gynandra*, herbaceous species (*T. aculeata*, *T. diffusa*, and *T. microcarpa*), and *Tarenaya* species (Spinosa I and II, Parviflorae, and Cleorosea) (**Supplementary Figure S5**). For the internal CO_2 concentration (C_i), which is related to g_s , the same pattern as that for g_s was observed (**Supplementary Figure S5**). Regarding transpiration (E) and R_d , the studied Cleomaceae accessions exhibited substantial differences with no clear pattern between the groups (**Figure 3** and **Supplementary Figure S5**). Similarly, WUE_i was remarkably higher in *G. gynandra*, albeit without a clear trend in the rest of the species (**Figure 3**).

Biochemical Analyses

To unveil the natural variations among the different Cleomaceae accessions studied, we performed detailed metabolite analyses using leaf samples. First, we examined the levels of the major carbon- and nitrogen-containing metabolites in leaves harvested at the middle of the light period. Overall, despite clear variations in physiological traits (**Figures 3E,F** and

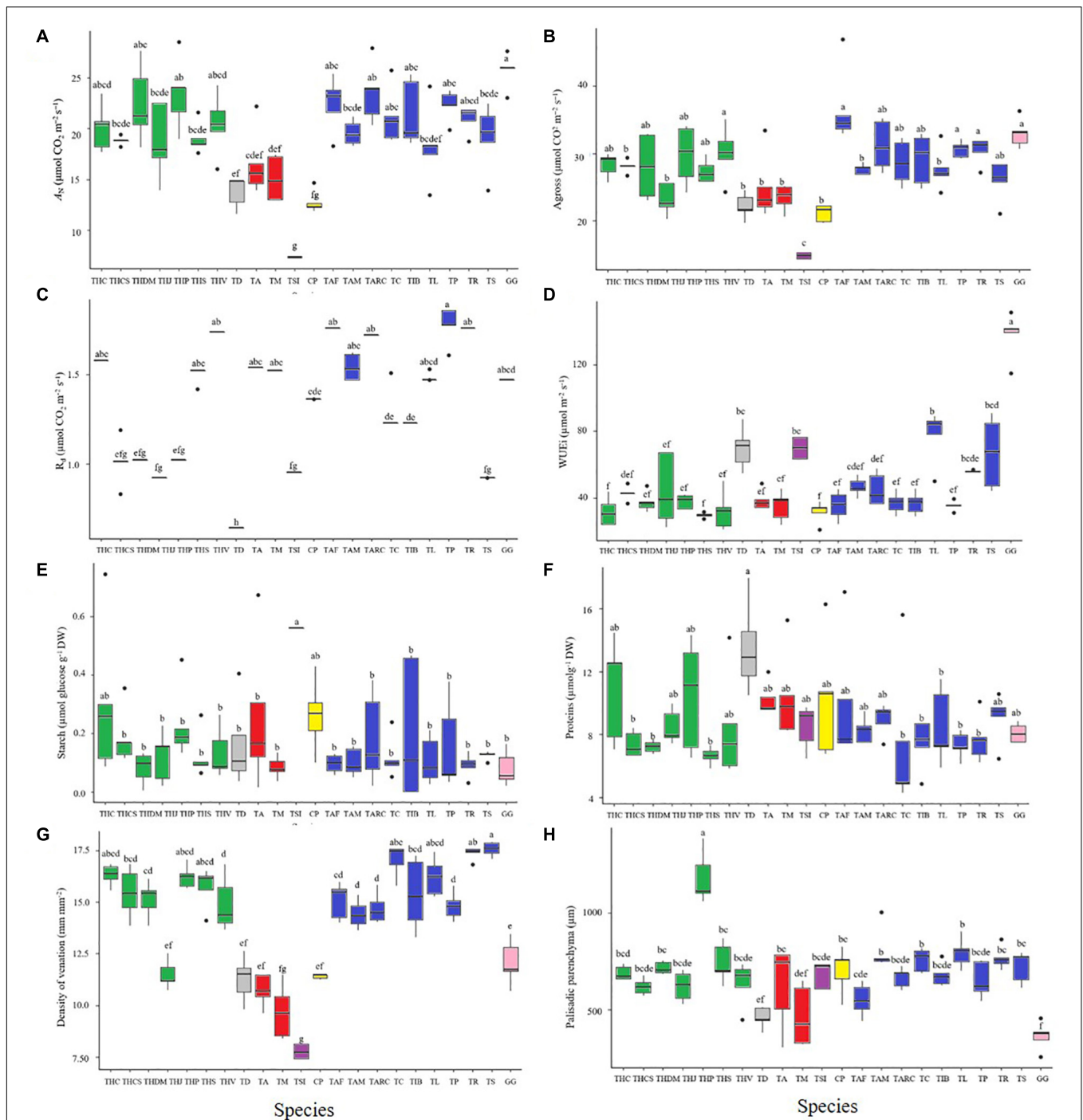


FIGURE 3 | Gas exchange and chlorophyll a fluorescence parameters in Cleomeaceae species. Physiological variables: **(A)** Ambient CO₂ assimilation rates (A_N) (400 ppm atmospheric [CO₂]). **(B)** Stomatal conductance (g_s). **(C)** Dark respiration (R_d). **(D)** Intrinsic water use efficiency (WUEi). Metabolic variables: **(E)** Starch content. **(F)** Protein content. Anatomical variable: **(G)** Density of venation. **(H)** Palisade parenchyma. Letters above individual box-scatter indicate significant groupings according to Tukey's Test ($n = 5$). The median is indicated by solid lines in each box; data dispersion is represented by the interquartile range, followed by standard error and outliers. The colored bars as well as the species acronyms are related to the groups observed in **Figures 1, 2**.

Supplementary Figure S6), the steady-state levels of soluble sugars (glucose, fructose, and sucrose), starch, amino acids, proteins, and chlorophylls did not differ among the plants of

different species (**Figures 3E,F** and **Supplementary Figure S6**). The only exception to this trend was *T. siliculifera*, which exhibited higher steady-state levels of sugars and starch than

TABLE 2 | Physiological variation for photosynthetic gas-exchange and anatomical parameters among diverse species of Cleomaceae, Brassicaceae, and Asteraceae.

Species	A_N ($\mu\text{mol m}^{-2}\text{s}^{-1}$)	$\delta^{13}\text{C}$ (‰)	Vein density (mm mm^{-2})	References
<i>Gynandropsis gynandra</i> – C ₄	23–35	–14 to 17	6–10	Marshall et al., 2007; Voznesenskaya et al., 2007; Koteyeva et al., 2011; Reeves et al., 2018
Cleomaceae	28	–15	11–12.5	Present study
<i>Tarenaya hassleriana</i> – C ₃	–	–24 to 30	–	Marshall et al., 2007; Voznesenskaya et al., 2007
Cleomaceae	18–24	–32	12–16	Present study
<i>Tarenaya spinosa</i> – C ₃	–	–26 to 30	5	Marshall et al., 2007; Voznesenskaya et al., 2007
Cleomaceae	20	–31	17	Present study
<i>Coalisina paradoxa</i> – C ₃ – C ₄	–	–	9–11	Marshall et al., 2007
Cleomaceae	18	–26	–	Voznesenskaya et al., 2007
<i>Arabidopsis thaliana</i> – C ₃	16	–	1.5–3	Stewart et al., 2018
Brassicaceae	10–16	–27 to 30	–	Easlon et al., 2014
<i>Moricandia moricandioides</i> – C ₃	28	–31 to 36	4–6	Schlüter and Weber, 2016
Brassicaceae				
<i>Moricandia suffruticosa</i> – C ₃ – C ₄	25	–31 to –33	3.5–4.5	
Brassicaceae				
<i>Moricandia arvensis</i> – C ₃ – C ₄	25	–30 to 37	4–6	
Brassicaceae				
<i>Flaveria robusta</i> – C ₃	–	–	2.65	McKown and Dengler, 2009
Asteraceae				
<i>Flaveria bidetins</i> – C ₄	–	–	2.89	
Asteraceae				

the other species (**Figure 3E** and **Supplementary Figure S6**). Meanwhile, *G. gynandra* exhibited higher levels of amino acids (**Figure 3E**) and proteins than *T. diffusa* (**Figure 3F**). There were no significant differences in the chlorophyll *a/b* ratio among the studied species (**Supplementary Figure S6**).

Furthermore, we performed metabolite profiling of leaf samples from all studied accessions using GC–MS. This analysis allowed for the identification and quantification of 33 metabolites (**Supplementary Table S3** and **Supplementary Figure S7**). For 19 metabolites analyzed, we did not observe significant differences among the studied accessions. Among these metabolites, there were no differences in the levels of the amino acids aspartate, glycine, and serine or the organic acids citrate and isocitrate. In contrast, *T. siliculifera* exhibited significantly higher levels of myo-inositol, succinate, malonate, malate, threonate, glycerate, glycerol, glucose, fructose, and sucrose. In addition, *T. hassleriana* exhibited higher levels of methionine, glutamate, and alanine.

Leaf Anatomy

In leaves, the formation of venation, plasmodesmata, and other barriers to gas diffusion is important for photosynthetic efficiency. Thus, the variability in leaf anatomical traits, which are related to the carbon concentrating mechanism, was determined in the Cleomaceae accessions studied. Leaf anatomical parameters were evaluated by diaphanization and transverse sectioning to determine VD and BSCW. *T. hassleriana* (THC, THCS, THP, and THS), *T. longicarpa* (TP, TC, and TIB), *T. rosea*, and *T. spinosa* showed higher VD than the other analyzed accessions (**Figure 3G**). Meanwhile, *T. hassleriana* (THDM and THV), *T. longicarpa* (TAF, TAM, and TARC), and

T. parviflora showed intermediate VD, whereas *G. gynandra*, *T. hassleriana* (THJ), *T. diffusa*, *T. aculeata*, *T. microcarpa*, *T. siliculifera*, and *C. paludosa* exhibited lower VD (**Figure 3G**).

Bundle sheath cell width was higher in *G. gynandra*, *T. hassleriana* (THC and THCS), *T. siliculifera*, and *T. longicarpa* (TAM) than in the other accessions studied (**Supplementary Figure S8**). Meanwhile, *T. diffusa*, *T. aculeata*, *T. microcarpa*, *T. parviflora*, and *T. longicarpa* (TARC and TAF) exhibited lower BSCW. The remaining 11 accessions exhibited intermediate BSCW (**Supplementary Figure S8**).

The interveinal distance (ID) was higher in *T. microcarpa* but lower in *G. gynandra* and *T. siliculifera*. The other accessions showed intermediate ID (**Supplementary Figure S8**). *T. hassleriana* (THP) showed the highest leaf thickness, whereas *T. diffusa* and *T. microcarpa* showed the lowest leaf thickness. The other accessions exhibited intermediate values and did not differ in terms of thickness (**Supplementary Figure S8**). Regarding the thickness of the palisade (**Figure 3H**) and spongy parenchyma (**Supplementary Figure S8**), *T. hassleriana* (THP) exhibited higher values and *G. gynandra* showed lower values than the remaining accessions, which showed intermediate values (**Supplementary Figure S8**).

Surprisingly, we could not separate the accessions into groups based on these morphoanatomical characteristics, which would be expected considering that the C₄ species *G. gynandra* could be clearly distinguished from the other C₃ species in terms of most of the analyzed parameters (e.g., VD and BSCW) (**Supplementary Figures S9, S10**). In this context, our results suggest that the analyzed accessions diversified at the species level. Since *T. hassleriana* and *T. longicarpa* differed in terms of the analyzed parameters, anatomy would provide additional evidence of this diversification. Although these

traits indicate the possible diversification in photosynthetic mechanisms, physiological and biochemical data provide additional evidence.

DISCUSSION

Interspecific Variations in the 2C Value Complement the Molecular Phylogeny of Cleomaceae

Cleomaceae is a highly diverse family, both morphologically (e.g., monoecious, dioecious, polygamous species; e.g., Omondi et al., 2017; Zohoungbogbo et al., 2018; Riaz et al., 2019) and physiologically (species with different photosynthetic metabolisms: C₃, C₃-C₄, and C₄). This diversity was represented by species studied here, which were morphologically (*Tarenaya*, *Cleoserrata*, and *Gynandropsis*; Stevens, 2001; Bercht and Presl, 2021) and physiologically (e.g., *Tarenaya* and *Gynandropsis*; Marshall et al., 2007; Bayat et al., 2018) distinct. The three genera analyzed here, namely *Tarenaya*, *Cleoserrata*, and *Gynandropsis*, were monophyletic (Figure 2). Of note, however, *Gynandropsis* is a monotypic genus (*G. gynandra*). *Tarenaya*, one of the most diverse genera in terms of the number of species within Cleomaceae, also includes many morphologically distinct species, which allows for the separation of the genus into series (small groups of species) (e.g., Iltis, 1957, 1959; Hall et al., 2002; Sanchez-Acebo, 2005; Inda et al., 2008; Feodorova et al., 2010; Iltis and Cochrane, 2014). These series have previously been shown to be monophyletic (see Soares-Neto et al., 2020), and our results are largely congruent with this report, with the exception of the *Spinosa* series, which we found to be polyphyletic. Of note, our study is limited by the number of samples of this rather diverse series (see Soares-Neto et al., 2020). Thus, studies with increased taxon sampling or markers are warranted to resolve the monophyly of the *Spinosa* series.

The morphological and physiological diversity can be linked to variations in genome size, among other factors (Paterson et al., 2010; Roddy et al., 2019). Thus, an interspecific variation at the diploid level, for example, as found for the species *T. hassleriana*, *T. diffusa*, *T. aculeata*, and *T. microcarpa*, may suggest that the DNA content may be a parameter that can be used to differentiate the species (e.g., *Miscanthus* 2C = 3.9 to 6.9 pg – Sheng et al., 2016). However, the observed species and genome size diversity was not consistent with the molecular phylogenetic results (Figure 2; Patchell et al., 2014; Bayat et al., 2018). This pattern is different, for example, from that observed for *Lupinus* (Fabaceae). In this genus, the genome size (0.97–2.44 pg) data supports the generally accepted taxonomic classification of the Old World lupins (Naganowska et al., 2003). In this sense, considering members of Cleomaceae, we observed that different series have species with the same genome size (*Parviflora*, *Rosea*, and *Spinosa*). Furthermore, within the same series it was also possible to observe representatives with different genome sizes (e.g., *T. hassleriana* and *T. spinosa* – *Spinosa* series, and *T. rosea* and *T. siliculifera* – *Rosea* series) (Figure 2). It is noteworthy that the studied Cleomaceae species have an average genome size of 0.5 – 2.2 pg, which is larger than that

recorded for *Arabidopsis*. However, in line to most species that have their genome quantified (Bai et al., 2012), such as rice, tomatoes and fruit-cherry, mango, papaya, orange, and peach (Arumuganathan and Earle, 1991).

Based on the variations in genome size among Cleomaceae genera and even among species of the same genus (e.g., *Tarenaya*; Figure 2A), even our small sample of the family reflects the relatively large interspecific variability. The intraspecific variations in the ITS sequence as well as the interspecific variations in this sequence and the 2C value may be related to different selective environmental pressures. Polyploidy, disploidy (ascendant and/or descendant), and genome size are associated with life-history traits, including vegetative form, flowering time, and adaptation to particular ecological niches, generating a basis for evolutionary novelty (Gregory, 2002; Chris Pires et al., 2006; Defoort et al., 2019). It is noteworthy that the species studied here have different forms of life (herbaceous vs. shrubby) and occur in different environments/biomes and consequently occupy different niches (Figure 1 and Supplementary Table S1). Nonetheless, only a few Cleomaceae species have been characterized in terms of their chromosome number (Ammal, 1933; Subramania and Susheela, 1988; Inda et al., 2008) and/or genome size (Omondi et al., 2017), and further efforts are required to understand the karyotype evolution in these taxa.

The events of gene/genome duplication observed for members of Cleomaceae contributed to several aspects of the evolution of C₄ photosynthesis in *G. gynandra* (Huang et al., 2021). Accordingly, this species has retained the duplicates of alanine aminotransferase and glutamine oxoglutarate aminotransferase. Besides almost all known vein-development-related paralogous genes derived from the genome duplication, this event also facilitated the evolution of C₄ enzyme genes and their recruitment into the C₄ pathway. In addition, several genes encoding photosystem I proteins were derived from the genome duplication (for more details see Huang et al., 2021). Furthermore, there are some examples of the duplication of gene copy number and its outcomes in the evolution of C₄ metabolism, such as the phosphoenolpyruvate carboxylase kinase gene families and the carbonic anhydrase genes (Wang et al., 2009). However, the number of enzymes required for C₄ metabolism is limited. In addition, the duplicated genes and other genomic regions often produce different effects (Lynch and Conery, 2003) and do not always result in functional innovation (Nielsen et al., 2005). In this context, some studies have proposed the involvement of parallel evolution in changes of gene expression and amino acid sequences (Christin et al., 2012a,b; Williams et al., 2012). Therefore, the *cis*-elements that direct cell specificity in C₄ leaves are present in C₃ orthologous genes recruited to the C₄ pathway, probably facilitating parallel evolution (Williams et al., 2012).

The 2C Value and Characteristics of Carbon Concentrating Mechanisms in Cleomaceae

The increase and/or decrease in DNA content can promote phenotypic changes in the biochemical,

anatomical, and physiological aspects of photosynthesis (Warner and Edwards, 1993; Vyas et al., 2007; Oa et al., 2011; Roddy et al., 2020). The importance of species relationships in trait-based studies is well appreciated in the field of comparative biology (Guy et al., 2019). Accordingly, *G. gynandra*, the species with C₄ photosynthesis, possesses a larger genome (Figure 2A). Nonetheless, a critical component in the study of adaptations is the identification of evolutionary correlations between phenotypic characteristics in phylogenetically close species (Adams, 2014). In this context, phylogenetic regression analysis provides a flexible analytical tool for assessing the degree of evolutionary association between variables while accounting for phylogeny (Adams, 2014).

The species with intermediate genome size (2C = 1.30 pg) (Figure 2A) had shorter ID and BSCW values, similar to the C₄ species *G. gynandra* (Figure 3 and Supplementary Figure S8). The lowest ID observed in *G. gynandra* can be attributed to the decline in the mesophyll (M) cell number, as verified, for instance, by Marshall et al. (2007) and Reeves et al. (2018), and size, which are considered essential for optimal C₄ function, since fewer M cells reduce the mean diffusion distance for C₄ metabolites (Hattersley, 1984; Khoshravesh et al., 2020). In addition, the enlargement of BSCs (equivalent to that in C₄ plants) is considered essential for C₄ function; as such, larger BSCs allow for a greater organelle volume and create larger vacuoles, serving as a barrier to facilitate CO₂ trapping in the sheath tissues (Von Caemmerer and Furbank, 2003; Khoshravesh et al., 2020). Consistent with previous reports, our results (Figure 2A) indicated that increase in the genome size affected leaf morphological and anatomical traits, in addition to physiological function (Roddy et al., 2020). Although the mechanism underlying the effect of genome size on cellular morphology remains unknown (Roddy et al., 2020), its effects on the vascular transport network, vessel size, and density have already been demonstrated (Maherali et al., 2009; Hao et al., 2013; De Baerdemaeker et al., 2018; Simonin and Roddy, 2018). In agreement, it has been suggested that genome size is a better predictor of guard cell size and stomatal density (Simonin and Roddy, 2018). Therefore, genome size can act as a first-order restriction on carbon gain, which directly affects the upper limit of allocation for growth, reproduction, and defense (Roddy et al., 2020).

Based on this premise, genome size may affect the tolerance of environmental changes related to latitude, altitude, temperature, precipitation, salinity, and desiccation (Grime and Mowforth, 1982; Otto and Whitton, 2000; Díez et al., 2013; Wang et al., 2018; Silva Artur et al., 2019; Zhang et al., 2019; Meyerson et al., 2020). Therefore, in habitats that can support high productivity and primary metabolic rates (e.g., Atlantic Forest and Amazon rainforest), species with smaller genomes (e.g., *T. hassleriana*, *C. paludosa*, and *T. microcarpa*; Supplementary Table S1) predominate, as they can maintain higher metabolic rates and rapidly adjust their physiology to match the environmental conditions (Simonin and Roddy, 2018; Roddy et al., 2020). It is thought to occur, since the genome size restricts the minimum cell size and the maximum cell compaction densities (Simova and Herben, 2012; Roddy et al., 2020). The increased cell

size represents a direct physical constraint on the number of cells that can occupy a given space and, as a result, on the distance between cell types and tissues. Furthermore, reductions in cell size, necessary to pack more veins and stomata into leaves, effectively bring actual primary productivity closer to its maximum potential (Simonin and Roddy, 2018). Thus, leaves with many small stomata and a high density of veins can maintain higher rates of gas exchange than leaves with fewer, larger stomata and larger, less numerous, veins (De Boer et al., 2012). Accordingly, variation in cell size can drive large changes in potential carbon gain (Simonin and Roddy, 2018). Regarding the effects of stress, environmental and physiological factors influence the final sizes of somatic eukaryotic cells. In this sense, the minimum size of meristematic cells and the rate of their production are strongly constrained by nuclear volume, more commonly measured as genome size (Simonin and Roddy, 2018). Meanwhile, arid habitats (e.g., Cerrado, Brazilian savanna, and Caatinga, Brazilian semi-arid region; Figure 1) are characterized by low productivity and can support species with large genomes (Roddy et al., 2020), such as *G. gynandra*, *T. spinosa*, and *T. longicarpa*, since a larger genome may be associated with greater genetic diversity (heterozygosity).

Although we hypothesize that genome size can predict the metabolic rate, its effects may be probably more nuanced, since numerous studies that have correlated the genome size with ecological factors have often produced conflicting results, and this correlation may change according to the group analyzed. Notably, studies addressing the diversity of genome size among closely related species and the association of genome size with phenotypes and ecological factors are scarce. In this light, the present study is the first to address variations in genome size within Cleomaceae, and further research is warranted to draw conclusions.

Are *Tarenaya* Species on an Evolutionary Trajectory Toward the C₃–C₄ Photosynthetic Mechanism?

C₄ photosynthesis arose from C₃ photosynthesis through a series of events/phases (Sage, 2004, 2021; Gowik and Westhoff, 2011). Combined physiological, molecular, and morphological changes played crucial roles in the evolution of the C₄ photosynthetic mechanism. The Cleomaceae accessions studied here were collected from warm and humid regions (Figure 1). For instance, *C. paludosa*, *T. microcarpa*, and most *T. hassleriana* accessions were collected from riverbanks in abandoned fields, except *T. hassleriana* (Joinville, SC), which was on an access road. The other species studied were collected from abandoned fields (*T. longicarpa* or *G. gynandra*). Similar to the species collected in the present study, some species with intermediate metabolism (e.g., *Flaveria linearis*; Holaday et al., 1984) grow in comparable environments and at disturbed sites, such as abandoned fields and roads. Thus, taking the steps essential for the development of the C₃–C₄ and C₄ photosynthetic mechanisms into account (see Sage, 2004; Gowik and Westhoff, 2011) and given that the studied Cleomaceae species occur in favorable environments (Figure 1) for the development of

the C₃–C₄ photosynthetic mechanism, our results suggest that *Tarenaya* species as well as *Cleoserrata* may be pre-conditioned to evolve the characteristics associated with carbon concentrating mechanisms. Similar trends have been observed in a previous study on *Cleome foliosa* and *Cleome africana* (Marshall et al., 2007), which exhibited increased VD and enlarged BSCs. These alterations incorporate some of the most important changes required for C₄ photosynthesis.

Some Cleomaceae species exhibit phenotypic plasticity in leaf development and cell biology (Table 2; Marshall et al., 2007; Reeves et al., 2018), and some species have already undergone gene duplication events (Schrantz and Mitchell-olds, 2006; Bergh et al., 2014). Furthermore, accessions of the same species (*T. hassleriana* and *T. longicarpa*) used in this study have a great genetic diversity, which can be observed by the different physiological, biochemical and anatomical data. This intraspecific diversity has already been observed for nine accessions of *G. gynandra* (Reeves et al., 2018) and can also be observed when comparing our accessions of *T. hassleriana*, *T. spinosa*, and *G. gynandra* with those from other continents (Table 2). However, modern phylogenetic methods allow us to analyze much more than just phylogeny as a statistical control. Specifically, they allow us to appreciate the evolutionary history of species, to better understand the patterns of biological diversity, to trace character traits over the evolutionary time, and to draw inferences regarding the evolution of these traits (Adams, 2014). As such, feature-based studies offer an important tool to better understand the ecological drivers of biological diversity. First, as observed in the present study, genome size was significantly correlated to variables essential for the C₄ photosynthetic mechanism, such as the $\delta^{13}\text{C}$ value, WUE_i, A_{gross}, A_N, malate, aspartate, starch, proteins, VD and size of palisade parenchyma (Table 1). As demonstrated for Grasses (Wang et al., 2009) and for *G. gynandra* (Huang et al., 2021) and reported in review papers (e.g., Monson, 2003; Sage, 2004, 2021; Gowik and Westhoff, 2011), the gene duplication or whole-genome duplication is thought to facilitate the evolution of C₄ photosynthesis from C₃ photosynthesis (e.g., Wang et al., 2009; Bianconi et al., 2018; Tronconi et al., 2020; Huang et al., 2021). The gene duplication or whole-genome duplication creates multiple copies of the gene, allowing for modification of the copies without the original function of the transcribed protein, so to reduce selective constraint and to acquire beneficial morphological or biochemical modifications (neofunctionalization) (Monson, 2003; Huang et al., 2021). It should be noted that gene duplications occur more frequently, since it is through sexual recombination, and thus are more likely to accumulate in short-lived annuals and perennials (Sage, 2004).

Furthermore, the second step in the development of the C₄ mechanism is characterized by increased VD (Sage, 2004; Gowik and Westhoff, 2011). The vascular system integrates with the photosynthetic tissues, and provides a flexible mechanical framework (Nelson and Dengler, 1997; Mckown and Dengler, 2010). In this way, in C₄ plants, the vascular system takes on an additional functional role, particularly C₄ biochemical cycling (Nelson and Dengler, 1997), due the ability to rapidly

assimilate and reduce CO₂, and survive conditions that promote the loss of carbon and energy to photorespiratory processes (Mckown and Dengler, 2010). In the present study, 15 accessions exhibited higher VD than the C₄ species *G. gynandra*; four accessions exhibited values similar to *G. gynandra* (as verified for two *Flaveria* species C₃ and C₄, which presented similar VD values – Table 2); and only two accessions exhibited values lower than *G. gynandra* (Figure 3G). Of note, the VD in *G. gynandra* was equivalent to that in other accessions of the species (6–10 mm.mm⁻²) (Marshall et al., 2007; Reeves et al., 2018). However, in the remaining C₃ accessions studied here, VD was higher than the previously reported values in the C₃ species *C. violaceae*, *C. isomeris*, *C. hirta*, and *C. africana* as well as the C₃–C₄ intermediate species *Coalisina paradoxa* (Marshall et al., 2007; Table 1). These values are too higher than those observed for Brassicaceae, *Arabidopsis* (C₃) and *Moricandia* (C₃ and C₃–C₄), and Asteraceae, *Flaveria* (C₃ and C₄) (Table 2).

Further, differences in VD observed in the present study may also be related to increase in the mechanical integrity of leaves, which may be beneficial in windy habitats or may improve water supply to leaves in dry and hot biotopes (Sage, 2004). The minor vein density, for example, is a key determinant of leaf hydraulic capacity and photosynthetic rates, and there would be strong benefit, independently of leaf size, in an ability to vary across a wide range of environments (Sack et al., 2012). In this regard, the characteristics that may initially be an adaptation to the environment, such as the combination of shorter ID, higher VD, and larger BSC, may predispose a species to developing the C₄ photosynthetic mechanism, as evidenced in grasses (Christin et al., 2013). Likewise, in Brassicaceae plants, VD has never been reported at the level of the C₄ species, indicating that this anatomical attribute may be one of the major constraints to the evolution of C₄ traits in this family (Schlüter et al., 2017). Therefore, increase in VD and enlargement of BSCs are the key alterations of foliar anatomy occurring in the C₃ context, preceding the emergence of the C₄ syndrome (Christin et al., 2013).

The third step in the development of the C₄ mechanism is marked by increase in the number of organelles in BSCs, resulting in cell enlargement. Although the activation of BSCs may be a secondary effect of increase in VD (Gowik and Westhoff, 2011), some accessions such as *T. hassleriana* (Canaã, MG, and Canoinhas, SC), *T. siliculifera*, and *T. longicarpa* (Manaus, AM) (Supplementary Figure S8) showed BSC size comparable to *G. gynandra*. The fourth step in the evolution of the C₄ mechanism is the appearance of glycine shuttling, a process in which the photorespiratory intermediate glycine is shuttled from the mesophyll tissue to the BSCs, where it is metabolized to CO₂ and serine by the action of glycine decarboxylase (Sage, 2004). Plants exhibiting this trait are considered C₃–C₄ intermediates because they present intermediate characteristics between the C₃ and C₄ mechanisms.

According to a previous carbon isotope discrimination analysis, *T. siliculifera* may present a modified photosynthetic mechanism (Voznesenskaya et al., 2007). However, in the

present study, the *T. siliculifera* accession exhibited a $\delta^{13}\text{C}$ value equivalent to the C₃ species, although anatomical and metabolic data indicated that it may be in transition from the C₃ to C₃–C₄ metabolism. Together, these results indicate that the studied *T. siliculifera* accession warrants further investigation, at both physiological and molecular levels, to define its photosynthetic metabolism.

CONCLUSION

Cleomaceae is a highly diverse family in which we can observe various types of photosynthetic metabolism, in addition to morphological differences. This diversity may be related to the evolutionary history of specific clusters, as distinct groups have different genome sizes, even within the same genus. However, this conclusion must be drawn with caution, because further evidence demonstrating that other C₄ species in the Cleomaceae group consistently have large genomes is essential. In the present study, we also demonstrated that the C₃-like species described here exhibit increases in VD and enlargement of BSCs, which may predispose these lineages to the development of C₄ photosynthesis.

DATA AVAILABILITY STATEMENT

The datasets presented in this study can be found in online repositories. The names of the repository/repositories and accession number(s) can be found in the article/**Supplementary Material**.

AUTHOR CONTRIBUTIONS

DP, MV, and AN-N designed the research, analyzed the data, and wrote the manuscript with input from all the others. DP performed most of the research with the support of MV, PF, and JS. WC, PW, US, WA, RV, MS, APMW, and AN-N provided technical, logistic, and financial support. All the authors contributed to the article and approved the submitted version.

FUNDING

This work was supported by funding from the Conselho Nacional de Desenvolvimento Científico e Tecnológico (CNPq; grant number 424024/2018-7) and the Fundação de Amparo à Pesquisa do Estado de Minas Gerais (FAPEMIG; grant numbers APQ-00528-18 and CRA-RED00053-16). The authors acknowledge the research fellowships granted by CNPq to AN-N and WA as well as the scholarship granted by Coordenação de Aperfeiçoamento de Pessoal de Nível Superior (CAPES) to DP. MV was supported by scholarships from CAPES (PNPD-1638006). APMW acknowledges funding from the Deutsche Forschungsgemeinschaft (DFG, German Research Foundation) under Germany's Excellence Strategy EXC-2048/1 (project ID 390686111) and by ERA-CAPS project C4BREED (WE2231/20-1).

ACKNOWLEDGMENTS

The authors thank the Instituto Estadual de Floresta (IEF) for the license granted (077/2017).

SUPPLEMENTARY MATERIAL

The Supplementary Material for this article can be found online at: <https://www.frontiersin.org/articles/10.3389/fpls.2021.756505/full#supplementary-material>

Supplementary Figure S1 | Scheme of how measurements were performed in the anatomical cross-section. PP, palisade parenchyma; SP, spongy parenchyma; T, leaf thickness; BSC, bundle sheath cell width; ID, internodal distance.

Supplementary Figure S2 | Molecular phylogeny of the Cleomaceae species sampled in this study. Bayesian Inference consensus tree inferred from sequences of nuclear ribosomal ITS. Numbers at nodes reflect PP. Bar: 0.02 nucleotide substitutions per site.

Supplementary Figure S3 | Evolutionary regression obtained from PGLS analysis (Brownian motion) conducted with 21 species. Only the variables that presented significant *P*-value (*P* < 0.05) are shown. Physiological variables: **(A)** Ambient CO₂ assimilation rates (A_N), **(B)** A_{gross}, **(C)** intrinsic water use efficiency (WUEi), and **(D)** respiration (R_d). Metabolic variables: **(E)** isotopic carbon composition ($\delta^{13}\text{C}$; •/••), **(F)** starch content, **(G)** protein content, and **(H)** Chlorophyll *a* + *b* content.

Anatomical variable: **(I)** palisade parenchyma and **(J)** density of venation. Growth parameter: **(K)** specific leaf area and **(L)** weight of 1000 seeds.

Supplementary Figure S4 | Evolutionary regression obtained from PGLS analysis (Brownian motion) conducted with 21 species. Only the variables more important that presented significant *P*-value (*P* < 0.05) are shown. Relative metabolite content from GC-MS. Amino acids A-H. **(A)** α -Alanine, **(B)** glutamine, **(C)** glycine, **(D)** leucine, **(E)** methionine, **(F)** phenylalanine, **(G)** proline, **(H)** serine. Organic acids **(I–K)**. **(I)** aspartate, **(J)** γ -aminobutyric – GABA, **(K)** malate. Sugars **(L)** glucose.

Supplementary Figure S5 | Gas exchange and chlorophyll *a* fluorescence parameters in Cleomaceae species. **(A)** Stomatal conductance (*g*_s), **(B)** Intern carbon (*C*_i), **(C)** Transpiration (*E*). Letters above individual box-scatter indicate significant groupings according to Tukey's Test (*n* = 5). The median is indicated by solid lines in each box; data dispersion is represented by the interquartile range, followed by standard error and outliers. The colored bars as well as the species acronyms are related to the groups observed in **Figures 1, 2**.

Supplementary Figure S6 | Levels of metabolites extracted from leaves of a subset of Cleomaceae species. For all metabolic analysis, leaf samples were harvested at middle of the day. **(A)** Glucose, **(B)** Fructose, **(C)** Sucrose, **(D)** Amino acids, **(E)** Chlorophyll *a*, **(F)** Chlorophyll *b*, **(G)** Chlorophyll *a* + *b*, **(H)** Chlorophyll *a/b*. Letters above individual box-scatter indicate significant groupings according to Tukey's Test (*n* = 5). The median is indicated by solid lines in each box; data dispersion is represented by the interquartile range, followed by standard error and outliers. The colored bars as well as the species acronyms are related to the groups observed in **Figures 1, 2**.

Supplementary Figure S7 | Heat map representing the changes in relative metabolite content in leaves collected at the middle of the day. Most species are 5 months old, except for TA, TM, TD, and GG which are 2 months old. The full data sets from these metabolic profiling are additionally available in **Supplementary Table S3**. GC-MS data was normalized by the mean of each species/metabolite. Letters indicate significant groupings according to Tukey's Test (*n* = 5). *Indicates not significant. The colored bars as well as the species acronyms are related to the groups observed in **Figures 1, 2**.

Supplementary Figure S8 | Natural variation of anatomical traits on leaves of a subset of Cleomaceae species. **(A)** Internodal distance, **(B)** Width bundle sheath cells, **(C)** spongy parenchyma, **(D)** Thickness. Letters above individual box-scatter indicate significant groupings according to Tukey's Test (*n* = 5). The median is indicated by solid lines in each box; data dispersion is represented by the

interquartile range, followed by standard error and outliers. The colored bars as well as the species acronyms are related to the groups observed in **Figures 1, 2**.

Supplementary Figure S9 | Vein density in leaves of Cleomaceae species. Spots indicate presence of secretory trichomes. **(A)** THC: *T. hassleriana* (Canaã-MG). **(B)** THCS: *T. hassleriana* (Canoinhas-SC). **(C)** THD: *T. hassleriana* (Domingos Martins-ES). **(D)** THJ: *T. hassleriana* (Joinville-SC). **(E)** THP: *T. hassleriana* (Piau-MG). **(F)** THS: *T. hassleriana* (São Miguel-MG). **(G)** THV: *T. hassleriana* (Viçosa-MG). **(H)** TD: *T. diffusa* (Feira de Santana-BA). **(I)** TA: *T. aculeata* (Feira de Santana-BA). **(J)** TM: *T. microcarpa* (Belém-PA). **(K)** TSI: *T. siliculifera* (Rio Pardo-MG). **(L)** CP: *C. paludosa* (Belém-PA). **(M)** TAF: *T. longicarpa* (Afrânio-PE). **(N)** TAM: *T. longicarpa* (Manaus-AM). **(O)** TARC: *T. longicarpa* (Arcoverde-PE). **(P)** TC: *T. longicarpa* (Lavras-CE). **(Q)** TIB: *T. longicarpa* (Ibimirim-PE). **(R)** TL: *T. longicarpa* (Picos-PI). **(S)** TP: *T. parviflora* (Pombal-PB). **(T)** TR: *T. rosea* (Colatina-ES). **(U)** TS: *T. spinosa* (Teresina-PI). **(V)** GG: *G. gynandra* (Mossoró-RN). The acronyms are followed by the species name and city/state of sampling state, between parenthesis. 10x. Bars = 10 μm.

Supplementary Figure S10 | Leaves cross section of Cleomaceae species. **(A)** THC: *T. hassleriana* (Canaã-MG). **(B)** THCS: *T. hassleriana* (Canoinhas-SC). **(C)** THD: *T. hassleriana* (Domingos Martins-ES). **(D)** THJ: *T. hassleriana* (Joinville-SC). **(E)** THP: *T. hassleriana* (Piau-MG). **(F)** THS: *T. hassleriana* (São

Miguel-MG). **(G)** THV: *T. hassleriana* (Viçosa-MG). **(H)** TD: *T. diffusa* (Feira de Santana-BA). **(I)** TA: *T. aculeata* (Feira de Santana-BA). **(J)** TM: *T. microcarpa* (Belém-PA). **(K)** TSI: *T. siliculifera* (Rio Pardo-MG). **(L)** CP: *C. paludosa* (Belém-PA). **(M)** TAF: *T. longicarpa* (Afrânio-PE). **(N)** TAM: *T. longicarpa* (Manaus-AM). **(O)** TARC: *T. longicarpa* (Arcoverde-PE). **(P)** TC: *T. longicarpa* (Lavras-CE). **(Q)** TIB: *T. longicarpa* (Ibimirim-PE). **(R)** TL: *T. longicarpa* (Picos-PI). **(S)** TP: *T. parviflora* (Pombal-PB). **(T)** TR: *T. rosea* (Colatina-ES). **(U)** TS: *T. spinosa* (Teresina-PI). **(V)** GG: *G. gynandra* (Mossoró-RN). The acronyms are followed by the species name and city/state of sampling state, between parenthesis. 10x. Bars = 10 μm.

Supplementary Table S1 | Description of the novel Brazilian species used for molecular phylogeny analyzes, and their respective collection sites (city-state abbreviation) and biomes.

Supplementary Table S2 | List of ITS sequences indicating species and its respective number of identification – accession number at NCBI – used for molecular phylogeny analyses.

Supplementary Table S3 | Relative metabolite content in leaves of Cleomaceae species sampled at middle of the day. Most species are 5 months old, except for TA, TM, TD, and GG, that are 2 months old. Data are presented as means ± SE. Letters indicate significant groupings according to Tukey's Test, $n = 5$.

REFERENCES

- Adams, D. C. (2014). A method for assessing phylogenetic least squares models for shape and other high-dimensional multivariate data. *Evolution (N. Y.)* 68, 2675–2688. doi: 10.1111/evo.12463
- Ammal, J. E. K. (1933). The chromosome number of *Cleome viscosa* Linn. *Curr. Sci.* 1933, 328–328. doi: 10.1016/B978-0-12-409548-9.10607-4
- Andrade-Lima, D. (1981). The caatingas dominium. *Revista Brasileira de Botânica.* 4, 149–163.
- Arumuganathan, K., and Earle, E. D. (1991). Nuclear DNA content of some important plant species. *Plant Molecular Biology Reporter.* 9, 208–218.
- Bai, C., Alverson, W. S., Follansbee, A., and Waller, D. M. (2012). New reports of nuclear DNA content for 407 vascular plant taxa from the United States. *Annals of Botany* 110, 1623–1629. doi: 10.1093/aob/mcs222
- Bayat, S., Schranz, M. E., Roalson, E. H., and Hall, J. C. (2018). Lessons from Cleomaceae, the sister of Crucifers. *Trends Plant Sci.* 23, 808–821. doi: 10.1016/j.tplants.2018.06.010
- Bercht, C., and Presl, J. (2021). *Flora do Brasil*. Available online at: http://floradobrasil.jbrj.gov.br/reflora/listaBrasil/ConsultaPublicaUC/BemVindoConsultaPublicaConsultar.do?invalidatePageControlCounter=1&idsFilhosAlgas=%5B2%5D&idsFilhosFungos=%5B1%2C10%2C11%5D&lingua=&grupo=5&familia=null&genero=&especie=&autor=&nomeVernaculo=&nomeCompleto=Cleomaceae+Bercht.+%26+J.Presl&formaVida=null&substrato=null&ocorreBrasil=QUALQUER&ocorrencia=OCORRE&endemismo=TODOS&origem=TODOS®iao=QUALQUER&estado=QUALQUER&ilhaOceanica=32767&domFitogeograficos=QUALQUER&bacia=QUALQUER&vegetacao=TODOS&mostrarAte=SUBESP_VAR&opcoesBusca=TODOS_OS_NOMES&loginUsuario=Visitante&senhaUsuario=&contexto=consulta-publica (accessed February 17, 2021).
- Bergh, E., Van Den Kùlahoglu, C., Bräutigam, A., Hibberd, J. M., Weber, A. P. M., Zhu, X., et al. (2014). Current Plant Biology Gene and genome duplications and the origin of C₄ photosynthesis: Birth of a trait in the Cleomaceae. *Curr. Plant Biol.* 1, 2–9. doi: 10.1016/j.cpb.2014.08.001
- Beric, A., Mabry, M. E., Harkess, A. E., Eric Schranz, M., Conant, G. C., Edger, P. P., et al. (2020). Surprising amount of stasis in repetitive genome content across the Brassicales. *bioRxiv*. [Preprint]. doi: 10.1101/2020.06.15.153296
- Beric, A., Mabry, M. E., Harkess, A. E., Brose, J., Schranz, M. E., Conant, G. C., et al. (2021). Comparative phylogenetics of repetitive elements in a diverse order of flowering plants (Brassicales). *G3*. 11; jkab140. doi: 10.1093/g3journal/jkab140
- Bianconi, M. E., Dunning, L. T., Moreno-Villena, J. J., Osborne, C. P., and Christin, P. A. (2018). Gene duplication and dosage effects during the early emergence of C₄ photosynthesis in the grass genus *Alloteropsis*. *J. Exp. Bot.* 69, 1967–1980. doi: 10.1093/jxb/ery029
- Bradford, M. M. (1976). A rapid and sensitive method for the quantitation of microgram quantities of protein utilizing the principle of protein-dye binding. *Anal. Biochem.* 72, 248–254. doi: 10.1006/abio.1976.9999
- Bräutigam, A., and Gowik, U. (2016). Photorespiration connects C₃ and C₄ photosynthesis. *J. Exp. Bot.* 67, 2953–2962. doi: 10.1093/jxb/erw056
- Brown, N. J., Parsley, K., and Hibberd, J. M. (2005). The future of C₄ research – maize. *Flaviera or Cleome? Trends Plant Sci.* 10, 215–221. doi: 10.1016/j.tplants.2005.03.003
- Von Caemmerer, S., Von Ghannoum, O., Pengelly, J. J. L., and Cousins, A. B. (2014). Carbon isotope discrimination as a tool to explore C₄ photosynthesis. *J. Exp. Bot.* 65, 3459–3470. doi: 10.1093/jxb/eru127
- Chris Pires, J., Maureira, I. J., Givnish, T. J., Systma, K. J., Seberg, O., and Chris, J. (2006). Phylogeny, Genome Size, and Chromosome Evolution of Asparagales. *Aliso* 22, 287–304.
- Christin, P. A., Besnard, G., Edwards, E. J., and Salamin, N. (2012a). Effect of genetic convergence on phylogenetic inference. *Mol. Phylogenet. Evol.* 62, 921–927. doi: 10.1016/j.ympev.2011.12.002
- Christin, P. A., Edwards, E. J., Besnard, G., Boxall, S. F., Gregory, R., Kellogg, E. A., et al. (2012b). Adaptive evolution of C₄ photosynthesis through recurrent lateral gene transfer. *Curr. Biol.* 22, 445–449. doi: 10.1016/j.cub.2012.01.054
- Christin, P. A., Osborne, C. P., Chatelet, D. S., Columbus, J. T., Besnard, G., Hodkinson, T. R., et al. (2013). Anatomical enablers and the evolution of C₄ photosynthesis in grasses. *Proc. Natl. Acad. Sci. U. S. A.* 110, 1381–1386. doi: 10.1073/pnas.1216777110
- Christin, P. A., Osborne, C. P., Sage, R. F., Arakaki, M., and Edwards, E. J. (2011a). C₄ eudicots are not younger than C₄ monocots. *J. Exp. Bot.* 62, 3171–3181. doi: 10.1093/jxb/err041
- Christin, P. A., Sage, T. L., Edwards, E. J., Ogburn, R. M., Khoshravesh, R., and Sage, R. F. (2011b). Complex evolutionary transitions and the significance of C₃–C₄ intermediate forms of photosynthesis in molluginaceae. *Evolution (N. Y.)* 65, 643–660. doi: 10.1111/j.1558-5646.2010.01168.x
- Cross, J. M., Von Korff, M., Altmann, T., Bartzetko, L., Sulpice, R., Gibon, Y., et al. (2006). Variation of enzyme activities and metabolite levels in 24 arabidopsis accessions growing in carbon-limited conditions. *Plant Physiol.* 142, 1574–1588. doi: 10.1104/pp.106.086629
- De Baerdemaeker, N. J. F., Hias, N., Van den Bulcke, J., Keulemans, W., and Steppe, K. (2018). The effect of polyploidization on tree hydraulic functioning. *Am. J. Bot.* 105, 161–171. doi: 10.1002/ajb2.1032
- De Boer, H. J., Eppinga, M. B., Wassen, M. J., and Dekker, S. C. (2012). A critical transition in leaf evolution facilitated the Cretaceous angiosperm revolution. *Na. Comm.* 3, 1–11. doi: 10.1038/ncomms2217
- Defoort, J., Van de Peer, Y., and Carretero-Paulet, L. (2019). The evolution of gene duplicates in angiosperms and the impact of protein-protein interactions and the mechanism of duplication. *Genome Biol. Evol.* 2019, evz156. doi: 10.1093/gbe/evz156

- Díez, C. M., Gaut, B. S., Meca, E., Scheinvar, E., Montes-Hernandez, S., Eguiarte, L. E., et al. (2013). Genome size variation in wild and cultivated maize along altitudinal gradients. *New Phytol.* 199, 264–276. doi: 10.1111/nph.12247
- Doyle, J. J., and Doyle, J. L. (1990). Isolation of plant DNA from fresh tissue. *Focus* 12, 13–15.
- Easlon, H. M., Nemali, K. S., Richards, J. H., Hanson, D. T., Juenger, T. E., and McKay, J. K. (2014). The physiological basis for genetic variation in water use efficiency and carbon isotope composition in *Arabidopsis thaliana*. *Photosynth. Res.* 119, 119–129. doi: 10.1007/S11120-013-9891-5
- Felsenstein, J. (1985a). Confidence limits on phylogenies: an approach using the bootstrap. *Evolution* 39, 783–791.
- Felsenstein, J. (1985b). Phylogenies and the comparative method. *American Naturalist* 125, 1–15.
- Feodorova, T. A., Voznesenskaya, E. V., Edwards, G. E., and Roalson, E. H. (2010). Biogeographic patterns of diversification and the origins of C₄ in Cleome (Cleomaceae). *Systematic Botany* 35, 811–826.
- Fernie, A. R., Roscher, A., Ratcliffe, R. G., and Kruger, N. J. (2001). Fructose 2,6-bisphosphate activates pyrophosphate: fructose-6-phosphate 1-phosphotransferase and increases triose phosphate to hexose phosphate cycling in heterotrophic cells. *Planta* 212, 250–263. doi: 10.1007/s004250000386
- Fiehn, O. (2007). Validated High Quality Automated Metabolome Analysis of *Arabidopsis Thaliana* Leaf Disks. *Concepts in Plant Metabolomics* 2007, 1–18. doi: 10.1007/978-1-4020-5608-6_1
- Gowik, U., and Bra, A. (2011). Evolution of C₄ Photosynthesis in the Genus *Flaveria*: How Many and Which Genes Does It Take to Make C₄? *Plant Cell* 23, 2087–2105. doi: 10.1105/tpc.111.086264
- Gowik, U., and Westhoff, P. (2011). The Path from C₃ to C₄ Photosynthesis. *Plant Physiology* 155, 56–63. doi: 10.1104/pp.110.165308
- Gregory, T. R. (2002). Genome size and developmental complexity. *Genetica* 115, 131–146. doi: 10.1023/a:1016032400147
- Grime, J. P., and Mowforth, M. A. (1982). Variation in genome size - an ecological interpretation. *Nature* 299, 151–153. doi: 10.1038/299151a0
- Gu, J., Weber, K., Klemp, E., Winters, G., Franssen, S. U., Wienpahl, I., et al. (2012). Identifying core features of adaptive metabolic mechanisms for chronic heat stress attenuation contributing to systems robustness. *Integr. Biol.* 4, 480–493. doi: 10.1039/c2ib00109h
- Guy, C., Thiagavel, J., Mideo, N., and Ratcliffe, J. M. (2019). Phylogeny matters: revisiting a comparison of bats and rodents as reservoirs of zoonotic viruses. *R. Soc. Open Sci.* 6:181182. doi: 10.1098/rsos.181182
- Hall, J. C., Sytsma, K. J., and Iltis, H. H. (2002). Phylogeny of Capparaceae and Brassicaceae based on chloroplast sequence data. *Am. J. Bot.* 89, 1826–1842. doi: 10.3732/ajb.89.11.1826
- Hao, G. Y., Lucero, M. E., Sanderson, S. C., Zacharias, E. H., and Holbrook, N. M. (2013). Polyploidy enhances the occupation of heterogeneous environments through hydraulic related trade-offs in *Atriplex canescens* (Chenopodiaceae). *New Phytol.* 197, 970–978. doi: 10.1111/nph.12051
- Hatch, M. D. (1988). C₄ photosynthesis: a unique blend of modified biochemistry, anatomy and ultrastructure. 895, 81–106.
- Hattersley, P. W. (1984). Characterization of C₄ Type Leaf Anatomy in Grasses (Poaceae). Mesophyll: Bundle Sheath Area Ratios. *Ann. Bot.* 53, 163–180. doi: 10.1093/oxfordjournals.aob.a086678
- Heckmann, D., Schulze, S., Denton, A., Gowik, U., Westhoff, P., Weber, A. P. M., et al. (2013). Theory Predicting C₄ Photosynthesis Evolution: Modular, Individually Adaptive Steps on a Mount Fuji Fitness Landscape. *Cell* 153, 1579–1588. doi: 10.1016/j.cell.2013.04.058
- Holaday, A. S., Lee, K. W., and Chollet, R. (1984). C₃-C₄ Intermediate species in the genus *Flaveria*: leaf anatomy, ultrastructure, and the effect of O₂ on the CO₂ compensation concentration. *Planta* 160, 25–32. doi: 10.1007/BF00392462
- Huang, C.-F., Liu, W.-Y., Lu, M.-Y. J., Chen, Y.-H., Ku, M. S. B., and Li, W.-H. (2021). Whole-Genome Duplication Facilitated the Evolution of C₄ Photosynthesis in *Gynandropsis gynandra*. *Mol. Biol. Evol.* 38, 4715–4731. doi: 10.1093/MOLBEV/MSAB200
- IBGE (2021). *Brazilian Institute of Geography and Statistics*. Available online at: <https://www.ibge.gov.br/> (accessed December 1, 2021).
- Iltis, H. H. (1957). Studies in the Capparidaceae. III. Evolution and Phylogeny of the Western North American Cleomoideae. *Ann. Missouri Bot. Gard.* 44, 77. doi: 10.2307/2394679
- Iltis, H. H. (1959). Studies in the capparidaceae—VI. Cleome sect. physostemon: taxonomy, geography and evolution. *Brittonia* 11, 123–162. doi: 10.2307/2805135
- Iltis, H. H., and Cochrane, T. S. (2014). Studies in the Cleomaceae VI: A New Genus and Sixteen New Combinations for the Flora Mesoamericana. *Novon: A Journal for Botanical Nomenclature* 23, 51–58. doi: 10.3417/2013017
- Inda, L. A., Torrecilla, A.P., Catala, A.P., and Ruiz-zapata, T. (2008). Phylogeny of *Cleome* L. and its close relatives *Podandrogynne* Ducke and *Polanisia* Raf. (Cleomoideae, Cleomaceae) based on analysis of nuclear ITS sequences and morphology. *Plant Systematics and Evolution* 274, 111–126. doi: 10.1007/s00606-008-0026-y
- Kadereit, G., and Freitag, H. (2011). Molecular phylogeny of Camphorosmeae (Camphorosmoideae, Chenopodiaceae): Implications for biogeography, evolution of C₄-photosynthesis and taxonomy. *Taxon* 60, 51–78. doi: 10.1002/tax.601006
- Khoshravesh, R., Stata, M., Busch, F. A., Saladié, M., Castelli, J. M., Dakin, N., et al. (2020). The Evolutionary Origin of C₄ Photosynthesis in the Grass Subtribe Neurachninae 1. *Plant Physiol.* 182, 566–583. doi: 10.1104/pp.19.00925
- Koteyeva, N. K., Voznesenskaya, E. V., Cousins, A. B., and Edwards, G. E. (2014). Differentiation of C₄ photosynthesis along a leaf developmental gradient in two Cleome species having different forms of Kranz anatomy. *J. Exp. Bot.* 65, 3525–3541. doi: 10.1093/jxb/eru042
- Koteyeva, N. K., Voznesenskaya, E. V., Roalson, E. H., and Edwards, G. E. (2011). Diversity in forms of C₄ in the genus *Cleome* (Cleomaceae). *Ann. Bot.* 107, 269–283. doi: 10.1093/aob/mcq239
- Lynch, M., and Conery, J. S. (2003). The evolutionary demography of duplicate genes. *J. Struct. Funct. Genomics* 3, 35–44. doi: 10.1007/978-94-010-0263-9_4
- Mabry, M. E., Brose, J. M., Blischak, P. D., Sutherland, B., Dismukes, W. T., Bottoms, C. A., et al. (2020). Phylogeny and multiple independent whole-genome duplication events in the Brassicales. *Am. J. Bot.* 107, 1148–1164. doi: 10.1002/ajb2.1514
- McKown, A. D., and Dengler, N. G. (2009). Shifts in leaf vein density through accelerated vein formation in C₄ *Flaveria* (Asteraceae). *Ann. Bot.* 104, 1085–1098. doi: 10.1093/AOB/MCP210
- Maherali, H., Walden, A. E., and Husband, B. C. (2009). Genome duplication and the evolution of physiological responses to water stress. *New Phytol.* 184, 721–731. doi: 10.1111/j.1469-8137.2009.02997.x
- Mallmann, J., Heckmann, D., Bräutigam, A., Lercher, M. J., Weber, A. P. M., Westhoff, P., et al. (2014). The role of photorespiration during the evolution of C₄ photosynthesis in the genus *Flaveria*. *Elife* 2014, 1–23. doi: 10.7554/eLife.02478
- Marshall, D. M., Muhaidat, R., Brown, N. J., Liu, Z., Stanley, S., Griffiths, H., et al. (2007). *Cleome*, a genus closely related to *Arabidopsis*, contains species spanning a developmental progression from C₃ to C₄ photosynthesis. *Plant J.* 51, 886–896. doi: 10.1111/j.1365-313X.2007.03188.x
- Mckown, A. D., and Dengler, N. G. (2007). Key innovations in the evolution of Kranz anatomy and C₄ vein pattern in *Flaveria* (Asteraceae). *Am. J. Bot.* 94, 382–389. doi: 10.3732/ajb.94.3.382
- Mckown, A. D., and Dengler, N. G. (2010). Vein patterning and evolution in C₄ plants. *Structure Et Développement* 88, 775–786. doi: 10.1139/B10-055
- McKown, A. D., Moncalvo, J. M., and Dengler, N. G. (2005). Phylogeny of *Flaveria* (Asteraceae) and inference of C₄ photosynthesis evolution. *Am. J. Bot.* 92, 1911–1928. doi: 10.3732/ajb.92.11.1911
- Meyerson, L. A., Pyšek, P., Lučanová, M., Wigginton, S., Tran, C., and Cronin, J. T. (2020). Plant genome size influences stress tolerance of invasive and native plants via plasticity. *Ecosphere* 11, 3145. doi: 10.1002/ecs2.3145
- Monson, R. K. (2003). Gene duplication, neofunctionalization, and the evolution of C₄ photosynthesis. *Int. J. Plant Sci.* 164, 368400. doi: 10.1086/368400
- Naganowska, B., Wolko, B., Śliwińska, E., and Kaczmarek, Z. (2003). Nuclear DNA Content Variation and Species Relationships in the Genus *Lupinus* (Fabaceae). *Annals of Botany* 92, 349–355. doi: 10.1093/aob/mcg145
- Nelson, T., and Dengler, N. G. (1997). Leaf vascular pattern formation. *Plant Cell* 9, 1121–1135.

- Nielsen, R., Bustamante, C., Clark, A. G., Glanowski, S., Sackton, T. B., Hubisz, M. J., et al. (2005). A scan for positively selected genes in the genomes of humans and chimpanzees. *PLoS Biol.* 3:0976–0985. doi: 10.1371/journal.pbio.0030170
- Nunes-Nesi, A., Carrari, F., Gibon, Y., Sulpice, R., Lytovchenko, A., Fisahn, J., et al. (2007). Deficiency of mitochondrial fumarase activity in tomato plants impairs photosynthesis via an effect on stomatal function. *Plant J.* 50, 1093–1106. doi: 10.1111/j.1365-313X.2007.03115.x
- Nylander (2004). *MrModeltest v2. Program Distributed by the Author*. Uppsala: Uppsala University.
- O'Brien, T. P., Feder, N., and McCully, M. E. (1964). Polychromatic staining of plant cell walls by toluidine blue O. *Protoplasma* 59, 368–373. doi: 10.1007/BF01248568
- Oa, N. D. C. W., Coate, J. E., Schlueter, J. A., Whaley, A. M., and Doyle, J. J. (2011). Comparative Evolution of Photosynthetic Genes in Response to Polyploid and. *Plant Physiol.* 155, 2081–2095. doi: 10.1104/pp.110.169599
- Omondi, E. O., Debener, T., Linde, M., Abukutsa-Onyango, M., Dinssa, F. F., and Winkelmann, T. (2017). Mating biology, nuclear DNA content and genetic diversity in spider plant (*Cleome gynandra*) germplasm from various African countries. *Plant Breed.* 136, 578–589. doi: 10.1111/pbr.12485
- Otto, F. (1990). DAPI Staining of Fixed Cells for High-Resolution Flow Cytometry of Nuclear DNA. *Methods Cell Biol.* 33, 105–110. doi: 10.1016/S0091-679X(08)60516-6
- Otto, S. P., and Whitton, J. (2000). Polyploid Incidence and Evolution. *Annu. Rev. Genet.* 34, 401–437. doi: 10.1146/annurev.genet.34.1.401
- Patchell, M. J., Roalson, E. H., and Hall, J. C. (2014). Resolved phylogeny of Cleomaceae based on all three genomes. *Taxon* 63, 315–328. Available online at: <http://www.jstor.org/stable/taxon.63.2.315>
- Paterson, A. H., Freeling, M., Tang, H., and Wang, X. (2010). Insights from the Comparison of Plant Genome Sequences. *Annu. Rev. Plant Biol.* 61, 349–372. doi: 10.1146/annurev-arplant-042809-112235
- Porra, R. J., Thompson, W. A., and Kriedemann, P. E. (1989). Determination of accurate extinction coefficients and simultaneous equations for assaying chlorophylls *a* and *b* extracted with four different solvents: verification of the concentration of chlorophyll standards by atomic absorption spectroscopy. *BBA - Bioenerg.* 975, 384–394. doi: 10.1016/S0005-2728(89)80347-0
- Posada, D., and Buckley, T. R. (2004). Model selection and model averaging in phylogenetics: Advantages of akaike information criterion and bayesian approaches over likelihood ratio tests. *Syst. Biol.* 53, 793–808. doi: 10.1080/10635150490522304
- Praça-Fontes, M. M., Carvalho, C. R., Clarindo, W. R., and Cruz, C. D. (2011). Revisiting the DNA C-values of the genome size-standards used in plant flow cytometry to choose the “best primary standards”. *Plant Cell Rep.* 30, 1183–1191. doi: 10.1007/s00299-011-1026-x
- Reeves, G., Singh, P., Rossberg, T. A., Sogbohossou, E. O. D., Schranz, M. E., and Hibberd, J. M. (2018). Natural variation within a species for traits underpinning C₄ photosynthesis. *Plant Physiol.* 177, 504–512. doi: 10.1104/pp.18.00168
- Riaz, S., Abid, R., Syed, A., Ali, S. A., Munir, I., and Kaiser, M. (2019). Morphology and seed protein profile for a new species of the genus *Cleome* L. (Cleomaceae) from Pakistan. *Protein Chem. Proteomics* 78, 102–106.
- Roddy, A., Thérout-Rancourt, G., Abbo, T., Benedetti, J., Brodersen, C., Castro, M., et al. (2019). The scaling of genome size and cell size limits maximum rates of photosynthesis with implications for ecological strategies. *bioRxiv* [Preprint]. doi: 10.1101/619585
- Roddy, A. B., Thérout-Rancourt, G., Abbo, T., Benedetti, J. W., Brodersen, C. R., Castro, M., et al. (2020). The scaling of genome size and cell size limits maximum rates of photosynthesis with implications for ecological strategies. *Int. J. Plant Sci.* 181, 75–87. doi: 10.1086/706186
- Rodeghiero, M., Niinemets, Ü, and Cescatti, A. (2007). Major diffusion leaks of clamp-on leaf cuvettes still unaccounted: How erroneous are the estimates of Farquhar et al. model parameters? *Plant, Cell Environ.* 30, 1006–1022. doi: 10.1111/j.1365-3040.2007.001689.x
- Sack, L., Scoffoni, C., McKown, A. D., Frole, K., Rawls, M., Havran, J. C., et al. (2012). Developmentally based scaling of leaf venation architecture explains global ecological patterns. *Nature Communications* 3, 837.
- Sage, R. F. (2001). Environmental and evolutionary preconditions for the origin and diversification of the C₄ photosynthetic syndrome. *Plant Biol.* 3, 202–213. doi: 10.1055/s-2001-15206
- Sage, R. F. (2004). The evolution of C₄ photosynthesis. *New Phytol.* 161, 341–370. doi: 10.1111/j.1469-8137.2004.00974.x
- Sage, R. F. (2021). Russ Monson and the evolution of C₄ photosynthesis. *Oecologia* 2021, 1. doi: 10.1007/S00442-021-04883-1
- Sage, R. F., Christin, P., and Edwards, E. J. (2011). The C₄ plant lineages of planet Earth. *J Exp Bot* 62, 3155–3169. doi: 10.1093/jxb/err048
- Sage, R. F., Khoshhravesh, R., and Sage, T. L. (2014). From proto-Kranz to C₄ Kranz: building the bridge to C₄ photosynthesis. *J. Exp. Bot.* 65, 3341–3356. doi: 10.1093/jxb/eru180
- Sanchez-Acebo, L. (2005). A Phylogenetic Study of the New World Cleome (Brassicaceae, Cleomoideae) on JSTOR. *Ann. Missouri Bot. Gard.* 92, 179–201.
- Schlüter, U., Bräutigam, A., Gowik, U., Melzer, M., Christin, P., Kurz, S., et al. (2017). Photosynthesis in C₃–C₄ intermediate *Moricandia* species. *J. Exp. Bot.* 68, 191–206. doi: 10.1093/jxb/erw391
- Schlüter, U., and Weber, A. P. (2016). The Road to C₄ Photosynthesis: Evolution of a Complex Trait via Intermediary States. *Plant Cell Physiol.* 57:CW009. doi: 10.1093/PCP/PCW009
- Schranz, M. E., and Mitchell-olds, T. (2006). Independent Ancient Polyploidy Events in the Sister Families Brassicaceae and Cleomaceae. *Plant Cell* 18, 1152–1165. doi: 10.1105/tpc.106.041111.1
- Schuler, M. L., Mantegazza, O., and Weber, A. P. M. (2016). Engineering C₄ photosynthesis into C₃ chassis in the synthetic biology age. *Plant J.* 2016, 51–65. doi: 10.1111/tpj.13155
- Sheng, J., Hu, X., Zeng, X., Li, Y., Zhou, F., Hu, Z., et al. (2016). Nuclear DNA content in *Miscanthus* sp. and the geographical variation pattern in *Miscanthus lutarioriparius*. *Sci. Rep.* 6:34342. doi: 10.1038/srep34342
- Shim, S.-H., Lee, S.-K., Lee, D.-W., Brilhaus, D., Wu, G., Ko, S., et al. (2020). Loss of Function of Rice Plastidic Glycolate/Glycerate Translocator 1 Impairs Photorespiration and Plant Growth. *Front. Plant Sci.* 10:1726. doi: 10.3389/fpls.2019.01726
- Silva Artur, M. A., Costa, M.-C. D., Farrant, J. M., and Hilhorst, H. W. M. (2019). Genome-level responses to the environment: plant desiccation tolerance. *Emerg. Top. Life Sci.* 3, 153–163. doi: 10.1042/etls20180139
- Simonin, K. A., and Roddy, A. B. (2018). Genome downsizing, physiological novelty, and the global dominance of flowering plants. *PLoS Biol.* 16:e2003706. doi: 10.1371/journal.pbio.2003706
- Simova, I., and Herben, T. (2012). Geometrical constraints in the scaling relationships between genome size, cell size and cell cycle length in herbaceous plants. *Proceedings of the Royal Society B.* 279, 867–875.
- Soares-Neto, R. L., Thomas, W. W., Vasconcellos Barbosa, M. R., and Roalson, E. H. (2020). Diversification of New World Cleomaceae with emphasis on *Tarenaya* and the description of *Iltisiella* a new genus. *Taxon* 69, 321–336. doi: 10.1002/tax.12231
- Stevens, P. F. (2001). *Angiosperm Phylogeny Website. Version 14, July 2017 [and more or less continuously updated since]*. Available online at: <http://www.mobot.org/mobot/research/apweb/orders/brassicalesweb.htm> (accessed February 27, 2021).
- Stewart, J. J., Polutchko, S. K., Demmig-Adams, B., and Adams, W. W. (2018). Arabidopsis thaliana Ei-5: Minor vein architecture adjustment compensates for low vein density in support of photosynthesis. *Front. Plant Sci.* 9:693. doi: 10.3389/fpls.2018.00693/BIBTEX
- Subramania, D., and Susheela, G. (1988). *Cytotaxonomical Studies of South Indian Cappariaceae*. Tokyo: Japan Mendel Society.
- Tronconi, M. A., Hüdig, M., Schranz, M. E., and Maurino, V. G. (2020). Independent recruitment of duplicated β-subunit-coding NAD-ME genes aided the evolution of C₄ photosynthesis in Cleomaceae. *Front. Plant Sci.* 11:572080. doi: 10.3389/fpls.2020.572080
- Von Caemmerer, S., and Furbank, R. T. (2003). The C₄ pathway: An efficient CO₂ pump. *Photosynth. Res.* 77, 191–207. doi: 10.1023/A:1025830019591
- Voznesenskaya, E. V., Koteyeva, N. K., Chuong, S. D. X., Ivanova, A. N., Barroca, J., Craven, L. A., et al. (2007). Physiological, anatomical and biochemical characterisation of photosynthetic types in genus *Cleome* (Cleomaceae). *Funct. Plant Biol.* 34, 247. doi: 10.1071/FP06287
- Voznesenskaya, E. V., Koteyeva, N. K., Cousins, A., and Edwards, G. E. (2018). Diversity in structure and forms of carbon assimilation in photosynthetic organs in *Cleome* (Cleomaceae). *Funct. Plant Biol.* 45, 983–999. doi: 10.1071/FP17323

- Vyas, P., Bisht, M. S., Miyazawa, S.-I., Yano, S., Noguchi, K., Terashima, I., et al. (2007). Effects of polyploidy on photosynthetic properties and anatomy in leaves of *Phlox drummondii*. *Funct. Plant Biol.* 34, 673. doi: 10.1071/FP07020
- Wang, L., Czedik-Eysenberg, A., Mertz, R. A., Si, Y., Tohge, T., Nunes-Nesi, A., et al. (2014). Comparative analyses of C₄ and C₃ photosynthesis in developing leaves of maize and rice. *Nat. Biotechnol.* 32, 1158–1165. doi: 10.1038/nbt.3019
- Wang, P., Moore, B. M., Panchy, N. L., Meng, F., Lehti-Shiu, M. D., and Shiu, S. H. (2018). Factors influencing gene family size variation among related species in a plant family, solanaceae. *Genome Biol. Evol.* 10, 2596–2613. doi: 10.1093/gbe/evy193
- Wang, X., Gowik, U., Tang, H., Bowers, J. E., Westhoff, P., and Paterson, A. H. (2009). Comparative genomic analysis of C₄ photosynthetic pathway evolution in grasses. *Genome Biol.* 10, R68. doi: 10.1186/gb-2009-10-6-r68
- Warner, D. A., and Edwards, G. E. (1993). Effects of polyploidy on photosynthesis. *Photosynth. Res.* 35, 135–147. doi: 10.1007/BF00014744
- White, T. J., Bruns, T. D., Lee, S. B., and Taylor, J. W. (1990). *Amplification and Direct Sequencing of Fungal Ribosomal RNA Genes for Phylogenetics*. Florida, FL: Academic Press, doi: 10.1016/b978-0-12-372180-8.50042-1
- Williams, B. P., Aubry, S., and Hibberd, J. M. (2012). Molecular evolution of genes recruited into C₄ photosynthesis. *Trends Plant Sci.* 17, 213–220. doi: 10.1016/j.tplants.2012.01.008
- Yang, H., Yu, Q., Sheng, W. P., Li, S. G., and Tian, J. (2017). Determination of leaf carbon isotope discrimination in C₄ plants under variable N and water supply. *Sci. Rep.* 7, 498–w. doi: 10.1038/s41598-017-00498-w
- Zhang, J., Wang, M., Guo, Z., Guan, Y., Guo, Y., and Yan, X. (2019). Variation in ploidy level and genome size of *Cynodon dactylon* (L.) Pers. along a latitudinal gradient. *Folia Geobot.* 54, 267–278. doi: 10.1007/s12224-019-09359-y
- Zohoungbogbo, H. P. F., Houdegbe, C. A., Sogbohossou, D. E. O., Tossou, M. G., Maundu, P., Schranz, E. M., et al. (2018). Andromonoecy in *Gynandropsis gynandra* (L.) Briq. (Cleomaceae) and effects on fruit and seed production. *Genet. Resour. Crop Evol.* 65, 2231–2239. doi: 10.1007/s10722-018-0687-5
- Zsögön, A., Alves Negrini, A. C., Peres, L. E. P., Nguyen, H. T., and Ball, M. C. (2015). A mutation that eliminates bundle sheath extensions reduces leaf hydraulic conductance, stomatal conductance and assimilation rates in tomato (*Solanum lycopersicum*). *New Phytol.* 205, 618–626. doi: 10.1111/nph.13084

Conflict of Interest: The authors declare that the research was conducted in the absence of any commercial or financial relationships that could be construed as a potential conflict of interest.

Publisher's Note: All claims expressed in this article are solely those of the authors and do not necessarily represent those of their affiliated organizations, or those of the publisher, the editors and the reviewers. Any product that may be evaluated in this article, or claim that may be made by its manufacturer, is not guaranteed or endorsed by the publisher.

Copyright © 2022 Parma, Vaz, Falquetto, Silva, Clarindo, Westhoff, van Velzen, Schlüter, Araújo, Schranz, Weber and Nunes-Nesi. This is an open-access article distributed under the terms of the Creative Commons Attribution License (CC BY). The use, distribution or reproduction in other forums is permitted, provided the original author(s) and the copyright owner(s) are credited and that the original publication in this journal is cited, in accordance with accepted academic practice. No use, distribution or reproduction is permitted which does not comply with these terms.